

# A Comprehensive Survey on Computer-Aided Diagnostic Systems in Diabetic Retinopathy Screening

Meysam Tavakoli<sup>a\*</sup>, Patrick Kelley<sup>b</sup>

<sup>a</sup>*Radiation Oncology Dept., University of Texas Southwestern Medical Center, Dallas, TX, USA*

<sup>b</sup>*Dept. of Physics, Indiana University-Purdue University, Indianapolis, IN, USA*

\*Correspondence's email address: [meysamtavakkoli@gmail.com](mailto:meysamtavakkoli@gmail.com) (Meysam Tavakoli)

To appear in: Photo Acoustic and Optical Coherence Tomography Imaging, Volume 3

Angiography: an application in vessel imaging, Book Chapter, IOP Publishing.

<https://dx.doi.org/10.1088/978-0-7503-2060-3ch12>

---

## Summary

Diabetes Mellitus (DM) can lead to significant microvasculature disruptions that eventually causes diabetic retinopathy (DR), or complications in the eye due to diabetes. If left unchecked, this disease can increase over time and eventually cause complete vision loss. The general method to detect such optical developments is through examining the vessels, optic nerve head, microaneurysms, haemorrhage, exudates, etc. from retinal images. Ultimately this is limited by the number of experienced ophthalmologists and the vastly growing number of DM cases. To enable earlier and efficient DR diagnosis, the field of ophthalmology requires robust computer aided diagnosis (CAD) systems. Our review is intended for anyone, from student to established researcher, who wants to understand what can be accomplished with CAD systems and their algorithms to modeling and where the field of retinal image processing in computer vision and pattern recognition is headed. For someone just getting started, we place a special emphasis on the logic, strengths and shortcomings of different databases and algorithms frameworks with a focus on very recent approaches.

---

## **Important Acronyms**

- **Diabetes Mellitus:** DM.
- **Diabetic Retinopathy:** DR.
- **Non-proliferation Diabetic Retinopathy:** NPDR. • **Proliferation Diabetic Retinopathy:** PDR.
- **Microaneurysm:** MA.
- **Haemorrhage:** HE.
- **Exudate:** EXs.
- **Cotton Wool Spots:** CWS.
- **Neovascularization:** NV.
- **Macular edema:** ME.
- **Field-of-View:** FOV.
- **Computer-Aided Diagnosis:** CAD.
- **Optic Nerve Head:** ONH.
- **Receiver Operating Characteristic:** ROC.
- **Area Under the Curve:** AUC.
- **k-Nearest Neighbor:** kNN.
- **Support Vector Machine:** SVM.
- **Neural Network:** NN.
- **Artificial Intelligence:** AI.
- **Machine Learning:** ML.
- **Deep Learning:** DL.
- **Convolution Neural Network:** CNN.
- **Recurrent Neural Network:** RNN.
- **Autoencoder:** AE.

## Contents

<b>1 Introduction</b> .....	4
1.1 Clinical Signs of Diabetic Retinopathy.....	5
1.2 Stages of Diabetic Retinopathy .....	6
1.3 Retinal Imaging and Databases .....	8
<b>2 Computer-Aided Diagnosis and Diabetic Retinopathy</b> .....	11
<b>3 Retinal Landmarks Detection</b> .....	15
3.1 Localization and Segmentation of Optic Nerve Head.....	15
3.1.1 Detection of Optic Nerve Head Center.....	16
3.1.2 Segmentation of Optic Nerve Head .....	17
3.2 Vessel Segmentation .....	19
3.3 Localization of the Fovea.....	23
3.3.1 Hybrid-based method.....	24
3.3.2 Positional constraints-based .....	24
<b>4 Detection of retinal lesions</b> .....	25
4.1 Microaneurysms and Haemorrhages Detection: .....	25
4.2 Exudates Segmentation .....	28
<b>5 Artificial Intelligence in Diabetic Retinopathy</b> .....	29
5.1 Overview of Deep Learning .....	31
5.1.1 Retinal Blood Vessel Segmentation.....	31
5.1.2 Optic Nerve Head Detection.....	32
5.1.3 Microaneurysms and Hemorrhages detection .....	32
5.1.4 Exudates Detection.....	33
<b>6 Conclusion</b> .....	35

## 1. Introduction

The rapidly rising Diabetes Mellitus (DM) is one of the major issues of our recent health care [1]. The number of people affected by DM continues to increase at an alarming rate [2, 3]. The World Health Organization estimates for the next 25 years the number of diabetic people to grow from 130 to 350 million [4]. In the same direction, in the time between 2000 to 2030 another source anticipates the spread of the DM population worldwide to increase from 2.8% to 4.4% [5]. The real catch is that just half of the diabetic people are noticed about the disease [6]. From medical aspect viewpoint, DM leads to serious late complications such as macro and micro vascular changes which cause Diabetic Retinopathy (DR), heart disease, and renal problems [7, 8]. In DM, because of insulin insufficiency there is incapacitated metabolism of glucose; this in turn leads to damages and complications in blood vessels [9]. According to a study in the United States, DM is among the five lethal diseases, and yet there is no treatment for it. In the same study, the total yearly expense to diagnose and treat DM in 2002 was estimated to be \$132 billion [10]. In fact, unmanaged DM and its complication leads to different malfunctions and death.

DR is a serious issue stemming from DM that affects the eye and is a main cause of vision loss and blindness [11, 12]. DR is the resulting condition specifically for these complications and damaged vessels lying in the tissue behind the retina [13]. Unfortunately so many cases of diabetes goes undiagnosed and the connection between diabetes and eye vision isn't common knowledge; patients with DM are 25 times more likely at risk of vision loss when compared with non-diabetic ones [14]. DR is often overlooked and detected too late, since it is a silent disease, and it may be diagnosed by the patient when the vascular abnormalities in the retina have progressed to a stage that its cure is complicated and sometimes unfeasible [15, 16]. Therefore, the most successful therapy for DR can be managed just in the early phases of that. Consequently, early detection of DR thru systematic screening is of critically important.

It is believed that the screening of diabetic people for the evaluation of DR potentially reduces the risk of blindness in these people by 50% [17]. The problem is however that, this would produce immense costs, due to the large number of examinations. Moreover, there are not enough specialists especially in rural areas to do these examinations [18]. Physical screening of DR to address the large and mounting number of DR cases is therefore not possible. Instead, automated systems based on image processing methods may help to overcome this issue [19]. It would be more beneficial and helpful if the initial steps of analyzing the retinal images and detecting all retinal lesions in the images can be computerized through a robust computer automated system. In this way, the automated system would allow for speedier identification of the telltale signs of DR

from the early onset of retinal lesions and notify the ophthalmologist for further assessment. This would allow more patients to be screened per year and for the ophthalmologists to better manage and direct their time on those priority patients who would have otherwise been overlooked or delayed in treating [20].

### 1.1. Clinical Signs of Diabetic Retinopathy

Now, before we start DR diagnosis the big question is *what are the revealing indications of DR?* There are several abnormalities in the retina that are manifestations of DR which are concisely described below.

1) Microaneurysms (MAs): They are the first visible sign of DR. They appear as small and round shape dots near tiny retinal blood vessels in retinal images [21]. The size of MAs usually ranges from  $10\mu m$  to  $125\mu m$  in diameter [22, 19].

2) Haemorrhages (HEs): A more severe level of DR is caused by retinal haemorrhages or leakage of weak capillaries and ruptured MAs into the surface of the retina [23]. They are defined as a red spot with different shapes, such as "dot", "blot" and "flame" [23, 21] and irregular margin and uneven density [24].

3) Hard Exudates (EXs): When the lipoproteins and other proteins are leaking because of the degradation or breakdown of the blood-retina barrier through abnormal retinal vessels, hard EXs appear [25]. They become visible as small yellowish-white patches with shrill borders [24]. They are often collocated in bulks or semicircular hoops and placed in the exterior layer of the retina [24].

4) Cotton Wool Spots (CWS): Also called soft exudates, they occur due to occlusion, or blockage of blood supply, of arterioles and cause disruption and damage to areas of tissue [26]. The ischemia of the retinal layer of nerve fiber caused by reduced blood flow to the retina changes the axoplasmic flow and leads to accumulation of axoplasmic residue in the retinal ganglion cell axons. The accumulation of this axoplasmic residue arise as fleecy yellowish-white lesions in the retinal nerve fiber layer known as Soft Exudates or CWS [26, 27].

5) Neovascularizations (NVs): The new blood vessels start to grow on the inner surface of the retina because of primarily the lack of oxygen. These new blood vessels push into the surrounding retinal space and are feeble and very often bleed into retinal cavity, effecting the eyesight [10, 28].

6) Macular edema (ME): It is recognized as the swelling of the macula, an area at the center of the retina. It is resulted in penetrance of abnormal capillaries in the retinal because of the fluid leakage or solutes around the macula [29, 30]. Eventually, it influences the central the eyesight [31].

Figures 1 and 2 show typical normal retinal images with its basic landmarks, and abnormal images with different signs and stages of DR.

### 1.2. Stages of Diabetic Retinopathy

According to the existence of the aforementioned of clinical signs, and the severeness/density of these signs [34] DR is categorized into four kinds including: mild, moderate, severe Non-Proliferative DR (NPDR), and PDR [35, 36, 24]. Respect to number of MAs and HEs, the NPDR is introduced as normal, mild, moderate, and sever DR [37].

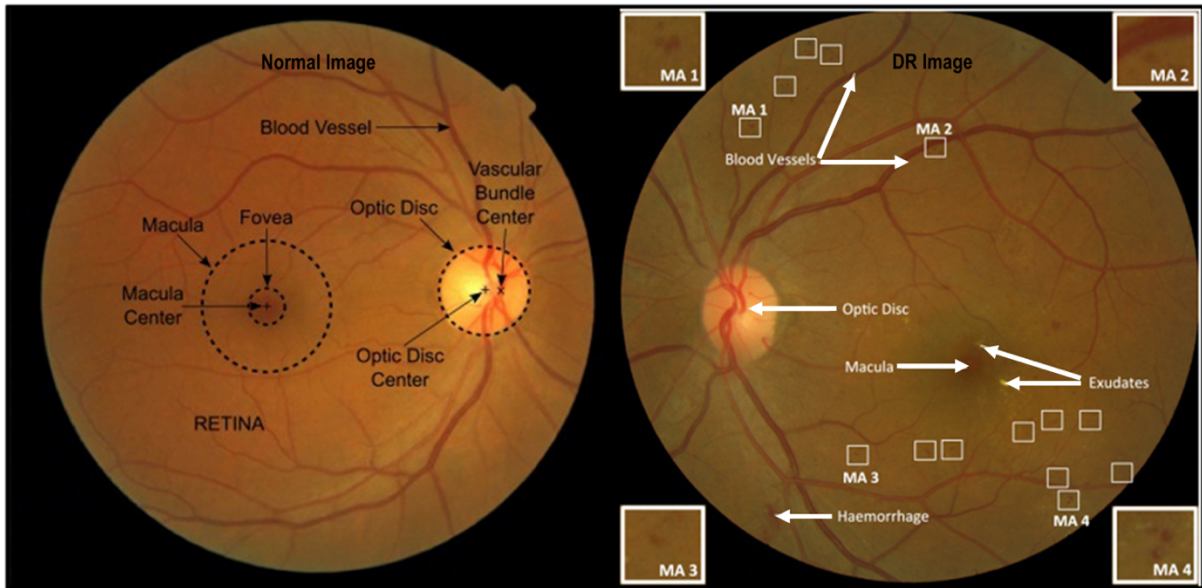


Figure 1: **Normal retinal image vs. DR one.** Sample retinal images for both normal and abnormal ones. On the left image, all available anatomical landmarks have been shown including fovea, macula, blood vessels, optic nerve head [32]. On the right one: there are all pathologic signs of DR including MAs, HEs, and EXs are visible [33].

- **Normal:** If no DR sign is observed.
- **Mild:** Here, only MAs are presented.
- **Moderate:** In this case, both MAs, and HEs are exist and their numbers are less than 20 in each quadrant, also we see soft EXs as well.
- **Severe:** Here, in each quadrant there are more than 20 MAs, and HEs. Also, in more than two quadrants there are some venous beadings and different shapes of hard EXs.

Figure 2 shows the retinal images of these categories and related signs. In the PDR, we see the initiation of new vessels, which are abnormal vessels (NVs). It is the severe phase of DR, in which these new abnormal vessel growth, caused by poor circulation especially from formations of MAs,

protrude into the retina and even into the vitreous, the gel-like medium that provides the eye its spherical shape. Thus, both MAs and NVs are two important clinical lesions [38] and fluid in DR is classified as EXs and non-EXs [39].

There are several organizations for DR grading such as American academy of ophthalmology, which classification of DR was established by curing of DR at its early stage [40], and protocol introduced by Scottish DR grading system [41]. Table 1 presents Scottish protocol.

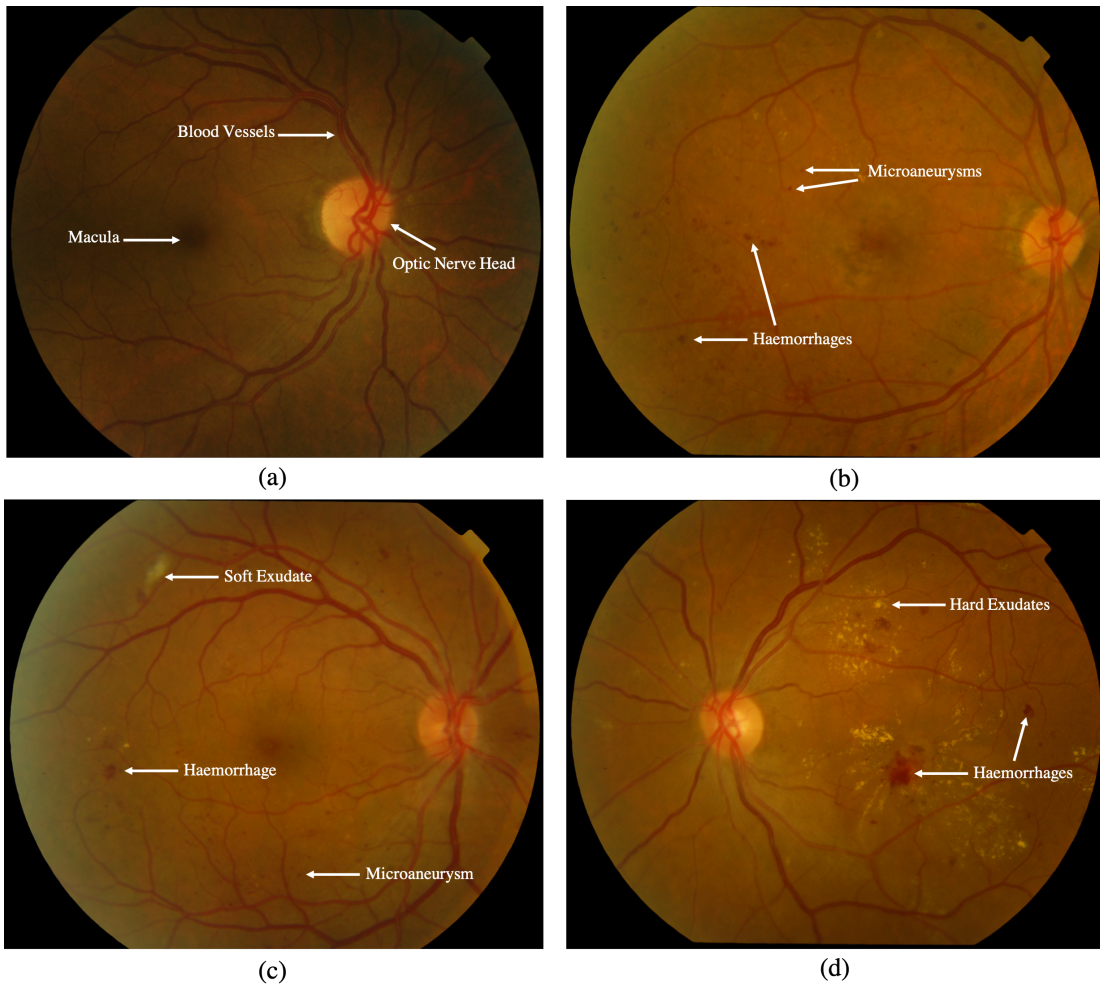


Figure 2: **Different types of DR.** (a) Normal; (b) Mild NPDR; (c) Moderate NPDR; (d) Severe NPDR.

Table 1: DR Scottish grading protocol [41].

Grade	Characteristics
No DR	Without abnormalities
Mild NPDR	Just MAs appear
Moderate NPDR	There are more than 5 MAs but less than severe NPDR
Severe NPDR	<ul style="list-style-type: none"> <li>- In each quadrant, there are more than 20 HEs</li> <li>- In two quadrants, there is Venous beading</li> <li>-Intra-retinal microvessel abnormalities</li> </ul>

PDR	-Any NVs at ONH or other parts of the retina -Vitreous/ pre-retinal HE
No ME	There are not any EXs or thickening of retina in posterior pole
Mild ME	There are EXs or thickening of retina at posterior pole, >1 disc diameters from fovea
Moderate ME	Same as mild ME's signs plus 1 disc diameters, without affecting fovea
Severe ME	There are EXs or thickening of retina with affecting fovea

MAs, in general, are very good indication of possibly worsening conditions of DR. From statistics point of view, the NPDR type with MAs has 6.2% chance to expand into PDR during a year [1]. An increased number of MAs is a main primary characteristic of DR progression. Moreover, with development of ischemia, there is an increased chance of PDR progress during first year. The first year risk growth increases from 11.3% (lower) to 54.8% (advanced) phase [1, 42]. In the NVs stage, diabetics have 25.6% to 36.9% chance of vision loss and blindness, if not cured appropriately. Furthermore, PDR eyes not therapied after more than 2 years have a chance of vision loss and blindness at 7.0% and if for more than 4 years it is not cured, the chance of vision loss goes up to 20.9%. On the other hand, this vision loss and blindness decreases to 3.2% during 2 years and 7.4% during 4 years of therapy [42]. Diabetic people with mild DR do not need specific treatment. In fact, they need to manage their DM and the related risk factors such as hypertension, anaemia, and renal malfunction. They require to closely be monitored, to decrease possibility of progressing higher stages of DR [18]. In the severe and advanced phase of DR, like NV, therapy is limited [43].

### 1.3. Retinal Imaging and Databases

Now that we are aware of the signs and stages of DR, the way diagnosis and determination of the stage of DR involves processing retinal images. Retinal photography is a procedure where 3-dimensional retinal landmarks is projected to the 2-dimension image. The created image shows the amount of reflected light [44]. In the camera which create the fundus image, the optical layout is equivalent to ophthalmoscope, which is used to observe the inner part of the eye. The camera sees the retinal area with 2.5 times magnification at the angle between 30° to 50°. More information can be found in [1]. In retinal photography for DR screening, the below modalities/techniques are utilizes [44].

1) Red-free retinal imaging: The image is taken by applying the amount of reflected light at a particular waveband.

2) Color retinal image: This image is based on Red Green Blue (RGB) spectrum and the camera detector sensitivity to the light.

3) Fluorescein angiography retinal image: The created image is based on the amount of photons that is emitted by fluorescein dye. The dye is injected through the blood stream [44].

Automated algorithms, in the process of testing and improving upon themselves, requires a set of exemplary data with the proper classifications. In our case, these would be retinal images from reputable databases, many of which have been classified by professional ophthalmologists. Most of the provided retinal images in these databases are used in application of screening and testing the proposed methods related to detection of MAs, HEs, exudates and other DR features. Outlined below, many of these online research databases are included. Table 2 summarizes all databases for detection of DR.

- **DIARTDB:** The dataset was created by Kauppi et al. [45] and is freely available for research from <http://www.it.lut.fi/project/imageret/>. Images were taken with a 50 degree field-of-view (FOV). It has two classes, DIARTDB0, including 130 color retinal images (20 images are normal without sign of DR and 110 contain symptoms of the DR). These signs include hard and soft EXs, MAs, HEs and NV. The second class is called DIARTDB1, including 89 images which 5 of them are normal and 84 ones contain at least mild NPDR signs (MAs).
- **HRF:** It is presented as the **H**igh-**R**esolution **F**undus retinal image dataset. The images were captured with different image acquisition setting and 45 degree FOV. In this database for each category of healthy, glaucomatous, and DR there are images. The information in database was created by a group of experts from the ophthalmology clinics [46].
- **STARE:** it consists of 400 images were initially applied by Hoover and Goldbaum [47]. These images were captured at 35 degree FOV.
- **KAGGLE:** The images were prepared by the Kaggle [37] as a series of high resolution ones. The images were captured under the different spatial conditions and were indexed by a well-experienced ophthalmologist respect to without DR to Mild, Moderate, Severe and Proliferative DR.
- **ROC: Retinopathy Online Challenge** is a dataset established for providing research groups to establish CAD system for diagnosis DR. It aimed to create a platform for algorithms evaluation [48].
- **DRIVE:** It has been developed from a DR screening system. The database included 40 retinal images in which 33 images without symptoms of DR and 7 ones showed signs of

DR. The database was taken using a non-mydrriatic 3CCD fundus camera with a 45 degree FOV [49].

- **MESSIDOR:** It consisted of 1200 eye retinal color images. The images were captured by a color non-mydrriatic retinography with a 45 degree FOV with different resolutions [50].
- **E-OPHTHA:** It was created because of a DR screening project which developed a color dataset for DR, called E-optha. This dataset was made of fundus images with variety of signs such as EXs and MAs which manually labelled by well-experienced ophthalmologists [51]. It contained 47 images with EXs, 35 with no sign, and 281 images with MAs or small HEs.
- **DRIONS:** An evaluating dataset for ONH segmentation that included 110 retinal images. The fundus images were captured with a color analogical camera [37].
- **CHASEDB1:** It is a dataset available at [blogs.kingston.ac.uk/retinal/chasedb1](http://blogs.kingston.ac.uk/retinal/chasedb1) for free. It included 28 fundus images. An ophthalmologist and human experts were asked to mark the vessels in all these images and these hand-labelled vessels were used as the ground truth (or gold standard) for this dataset [52].
- **HEI-MED:** The database is a test database for evaluating algorithms in the EXs and macular edema detection. It contained 169 images which were segmented manually by a high skilled ophthalmologist [30].
- **Others:** These are other datasets established by individual researchers groups such as MUMS-BD [19, 53] DMED, ARIA, Eyepack [1]

Table2: More details for the databases use for DR detection system

Database	Numbers	Resolution	Format	Task
MESSIDOR [50]	1200	1440x960, 2240x1488, 2304x1536	TIFF	-DR grading -Risk of DME
Kaggle [54]	80000	-	JPEG	-No sign of DR -Mild -Moderate -Severe -PDR
E-optha[55]	148 MAs, 233 normal, 47 EXs, 35 no signs of DR	2544x1696 1440x960	JPEG	-MA small HE detection -EX detection
DRIVE [49]	33 normal 7 mild DR stage	584x565	TIFF	-Vessels extraction
STARE [47]	402	605x700	PPM	-13 retinal diseases

				-Vessels segmentation -ONH
DIARETDB1[45]	5 no sign 84 NPDR symptom	1500x1152	PNG	-MAs -HEs
CHASE [37, 56]	28	1280x960	JPEG	-Vessels extraction
MUMS [19, 53]	120		PNG	MAs
ARIA [57]	16 normal 92 AMD- 59 DR	768x576	TIFF	-ONH -Fovea -Vessel
SEED-DB [58]	192 normal 43 glaucomatous	3504x2336	-	ONH
EyePACS [59]	9963	-	-	-Referable DR -MA
ORIGA [60]	482 normal 168 glaucomatous	720x576	-	ONH

Table 3 summarizes some CAD systems at different image database analysis for DR detection. These approaches are distinguished based on features, processing, and classification of DR.

*Table 3: Some CAD systems and databases(Blue=B, Green=G, Red=R)*

Author	Image plan	Method	database
Pourreza et al. [53]	B & G	Radon transformation	DRIVE, STARE, MUMS-DB
Esmaeili [61]	R& G	Morphology	STARE, DRIVE, DIARETDB1
Qureshi et al. [62]	G	Entropy and Hough	DIARETDB0, DIARETDB1, DRIVE
Welfer et al. [63]	LUV	Mathematical Morphology	DRIVE, DIARETDB1
Harangi and Hajdu [64]	Grey	Probabilistic model and augmented Naive based	DIARETDB0, DIARETDB1, DRIVE, MESSIDOR
Akyol et al. [65]	G	BLP	DIARETDB1, DRIVE,ROC
Dai et al. [66]	Grey	Hough, PCA	MESSIDOR, DRIONS
Alshayegi et al. [68]	Grey	Adaptive edge detection,	DERIVE, DMED, STARE, DIARETDB1
Fraz et al. [68]	G	Watershed transformation	DRIVE, Shifa, CHASEDB1, DIARETDB1

## 2. Computer-Aided Diagnosis and Diabetic Retinopathy

As previously mentioned, manual detection and diagnosis is an exhaustive task in both cost and lack of experts [16] when screening DR. It would be more cost effective and helpful if the initial task of analyzing the retinal images can be automated. Automated approaches address these issue by decreasing the time, expense, and attempt considerably [69]. Moreover, since image processing techniques are growing in all areas of medical science, by assisting them, especially in advanced ophthalmology, we can do automated screening [39].

For this reason, automated DR detection and classification utilizes Computer Aided Diagnostic (CAD) systems. These computer-based systems have the ability to detect any change in normal and abnormal images and systematize these variations to form a feature space. At the end, the mixture of these features introduces type and stage of DR. Different CAD systems have been presented in state of arts for early DR detection and related lesions [12, 18, 19, 70-77].

Normally, each CAD system is the sequence of two different approaches i.e. feature detection and a classification [37]. Since there are many different approaches in CAD systems, it is also necessary to evaluate their robustness and accuracy. There are many different standard methods used in assessing the effectiveness of the CAD systems. A common one is using Receiver Operating Characteristic (ROC) analysis and concept of area under the curve (AUC) analysis. The AUC of ROC curve is a measurement of performance for automated method, for example, extraction problem, at different thresholds values. ROC is a probability curve and AUC shows degree or rate of distinguishability. In fact, AUC shows us how much the method is able to distinguish between classes. Higher the AUC, better the method is in its prediction. By analogy, higher the AUC, better the method is at distinguishing between images with DR and no DR. ROC curves illustrate the tradeoff between sensitivity and specificity for a range of thresholds and enable the identification of an optimal value [78]. Hence, assessment using the ROC curve is a way to evaluate the model, independent of the choice of a threshold.

Here, the analytical definition when using ROC is assessed according to the true positive fraction (TPF), given by sensitivity, and the false positive fraction (FPF), (1-specificity) [16]. Moreover, the accuracy is specified as a quantification including the ratio of well-classified pixels. The final outputs for the automated approach as compared to the ground truth or gold standard are calculated for each image. These metrics are defined as:

$$\begin{aligned}
 \text{Sensitivity}(Se) &= \frac{TP}{TP + FN} \\
 \text{Specificity}(Sp) &= \frac{TN}{TN + FP} \\
 \text{Accuracy}(Acc) &= \frac{TP + TN}{TP + FN + TN + FP}
 \end{aligned} \tag{1}$$

where TP is true positive, TN is true negative, FP is false positive and FN is false negative same as in [79, 80].

A look into the results for both ROC and AUC (Eq. 1) obtained by others CAD systems in DR screening. Table 4 summarizes some of the algorithms at different image analysis for detection of DR.

Table 4: Some of the CAD systems with different image analysis stages

CAD system	Methodology	Authors
ONH detection and segmentation		Qureshi et al. [62], Welfer et al. [63], Harangi and Hajdu [64], Akyol et al. [65], Dai et al. [66], Alshayegi [67], Basit and Fraz [68], Bharkad [81], Lesay et al. [82], Zou et al. [83], Xiong and Li [84], Sarathi et al. [85], Lu [86], Lowel et. [87], Hoover et. [88]
Vessel segmentation	Thresholding approach,	Hoover et al. [47], Dash and Bhoi [89], Zhu et al. [90], Neto et al.[91], Xu and Luo [92], Nguyen et al. [93], Zhang et al. [94], Fraz et al. [95], Marin et al. [96], Akram et al. [97], Vermeer et al. [98], chakraborti et al. [99], Wu et al. [100], Tavakoli et al. [101], Roychowdhury et al.[102], Tolia and Panas [103], Azzopardi et al. [104], Zana et al. [105, 106], soares et al. [107]
	Tracking approach,	
	Machine classifiers	
Lesion detection	Red lesions (MAs, HEs)	Quelleg et al. [108], Walter et al. [22], Tavakoli et al. [19], Wang et al. [109], Srivastava et al. [110], seoud et al [23], Pereira et al. [113], Dai et al. [111], van Grinsven et al. [112]
	Hard and soft exudates	Liu et al. [114], Zhang et al. [116], Orlando et al. [115], Youssef and Solouma [117], Fraz et al. [118], Amin et al. [119], sopharak et al. [120], Sanchez et al. [121]
DR detection and classification	DR, Non DR NPDR, PDR	Tavakoli et al. [19], Koh et al. [122], Gardner et al.[123], Rubini and Kunthavai [124], Gulshan et al. [125], Kose et al. [126], Yang et al. [127], Sisodia et

		al. [128] , Kumar et al. [129], Gupta et al.[130], Leontidis [82], Sinthanayothin et al. [131], Usher et al. [132], Fleming et al. [17, 133], Perumalsamy et al. [134], Winder et al. [135], Mookiah et al. [136]
--	--	---

Briefly, both Tavakoli et al. [19] and Philip et al. [36] introduced a DR screening system based on the comparison of automated system respect to the gold standard which was manual detection by ophthalmologist. Their approach detected DR images with an accuracy of more than 90%. Sinthanayothin et al. [131] established a trustable automatic DR online screening system purposed to simplify ophthalmologists' work in their country. They got sensitivity and specificity for their screening program to classify the DR 80.2% and 70.7% respectively. Usher et al. [132] employed DR screening tool which detected DR with both sensitivity and specificity of 95.1% and 46.3% respectively. Niemeijer et al. [70] introduced a DR detection algorithm based on information fusion approach with AUC of 0.88. Quellec et al. [71] established an automated DR screening system for both MAs and age-related macular degeneration detection, and their method reached to an AUC of 0.93. Fleming et al. [133] introduced a CAD system to detect blot HEs and provided with both sensitivity and specificity of 98.60% of 95.50% respectively. Fleming et al. [17] also established another CAD system to detect MAs which got a sensitivity and specificity of 85.4% and 83.1%. Perumalsamy et al. [134] employed a CAD system and obtained an accuracy of 81.3% by evaluating the performance with ophthalmologists' idea. Abramoff et al. [137] established a web-based DR detection system with specific protocol and short questionnaire, measurement of visual eyesight, and four retinal images. The accuracy of their protocol reached 93%. Abramoff et al. [138] also presented an automated DR detection system which acquired an AUC of 0.84 of DR detection.

There are also some authors that reviewed most of the CAD methods, and their applications [1, 39, 44, 135, 139] for automated screening of DR. Winder et al. [135] discussed different segmentation approaches of Optic nerve head (ONH), retinal vessels, macula, and DR detection. Teng et al. [139] for retinal landmarks, and lesions segmentation, and image registration reviewed different methods. Abramoff et al. [44] surveyed various retinal imaging modalities, vessel segmentation, lesion, and ONH detection. Patton et al. [39] discussed image preprocessing, and registration methods, besides landmarks and lesions segmentation. Mookiah et al. [1] comprehensively reviewed the approaches to detect and extract the retinal lesions and landmarks such as ONH, vessels, EXs, MAs, and HEs.

From classification viewpoint, color characteristics were utilized on Bayesian classifier to group each pixel into either lesion or non-lesion categories [140]. In this study, authors obtained 100% accuracy in detection of all EXs in the retinal images, and accuracy of 70% in classification of normal retinal images. By using image processing techniques and multilayer Neural Network (NN), DR and normal retina were categorized with sensitivity and a specificity of 80.2% and 70.7% respectively [21]. Automated detection of NPDR, based on MAs, HEs, and EXs was studied in [136, 141]. The approach was able to correctly detect the NPDR stage with an accuracy of 81.7%. For DR screening again above lesions were used [142] and obtained the sensitivity and specificity of 74.8% and 82.7%, respectively. An early automated DR detection system was developed by Kahai et al. based on decision support system [143]. In their method, Bayes optimality criteria was used to identify DR with a sensitivity and specificity of 100% and 67%. Different stages of DR were grouped using both area and geometry of the combination of the vessels with a feedforward NN [144]. The average classification efficiency for this method was 84% with both sensitivity and specificity of 90% and 100%. Nayak et al. employed EXs and vessel area along with parameters related to its texture which coupled with NN to classify NPDR, PDR, and normal [5]. They got accuracy of 93%, sensitivity 99%, and specificity of 100%. The feature of support vector machine (SVM) classifier also used by Acharya et al. [145] to classify the retinal image in to normal, mild, moderate, severe and PDR categories. They showed a classification accuracy of 82% with sensitivity of 82%, and specificity of 88%. Nicolai et al. established an automated lesion detection algorithm for DR screening purpose, which detected 90.1% of diabetics and 81.3% of those without DR [146]. Their system showed both sensitivity and a specificity of 93.1% and 71.6%.

### **3. Retinal Landmarks Detection**

A standard CAD screening system needs to extract the retinal landmarks such as fovea, ONH, and vessels, and additionally lesions such as MAs, HEs, EXs, CWS, and NVs. Several studies have worked on various detection and segmentation approaches to identify these anatomical regions. Here, we briefly discuss them.

#### *3.1. Localization and Segmentation of Optic Nerve Head*

The ONH can reveal critical eye disease like glaucoma [147]. The shape of the ONH appears as semicircle or ellipse in the retinal image. The ONH is also applied as a reference landmark to identify other retinal regions and structures such as the macula and fovea [87, 148, 149, 150]. Moreover, the ONH localization assists to determine central retinal arteries and veins [87, 151]. Many vessel tracking algorithms use the ONH center as the starting point, since the vessels diverge from the ONH center. The ONH localization is carried out by detecting its center or by drawing a circle around the ONH region [152-156]. ONH segmentation is introduced by specifying the

boundary of ONH. Thus, identification and extraction of ONH is highly important [135, 147, 157-161].

The localization of the ONH is serious to differentiate it from the other lesions. The ONH identification approaches, as explained in literature mainly estimate its center or surround it by a circular mask. In both cases, the localization is quite an elaborate task because of the presence of thick vessels, inaccurate boundaries, and lesions such as EXs [135, 147]. The methods according to intensity changes are easy to use, fast and robust for images with no symptoms. These methods may lose when the ONH is concealed by blood vessels and lesions such as EXs, CWS, or other same intensity artifacts [162].

### *3.1.1. Detection of Optic Nerve Head Center*

The ONH color and shape can be utilized to detect it. Normally, in some studies the ONH is localized by its relations to bright pixel clusters. Sinthanayothin et al. [163] used a window size  $80 \times 80$  pixel as the size of a typical ONH and localized the ONH by observing the maximum change in its intensity to its neighboring pixels. They chose the point with highest pixel variance to detect the center of the ONH and reported a sensitivity and specificity of 99.1%. Lowel et al. [87] developed correlation filter to identify the ONH in presence of EXs and other artifacts and correctly detect it in 83% of cases. Hoover et al. [88] presented an approach using the concept of fuzzy approach to locate the ONH. Their approach obtained 89% correctly ONH detection. Walter et al. [164] introduced a method to detect ONH based on its illumination, distance, and watershed transformation in different color space, HSL (Hue, Saturation, Luminance), with accuracy of more than 85%. Tavakoli et al. applied three different vessel segmentation algorithms, Laplacian-of-Gaussian, Canny, and Matched filter edge detectors to detect the ONH in both the images without DR signs and in the presence of DR [165].

The Hough and similarly the Radon transform were applied by many authors to identify the ONH [53, 87, 166-168]. The method is based on integral transformation, or mapping the values of the line integral of an images pixels into another domain. Ultimately, the ONH was identified by effective projection profiles in Radon space and the boundary parts with maximum vote [53].

Principal Component Analysis (PCA) was another method for identifying the ONH ([163, 169, 170]). In fact, this method turns the correlated variable into uncorrelated ones which is known as principle parts [1]. The first principal component demonstrates the maximum information exist in the image. Li and Chutatape [170] detected the ONH using the concept of PCA with accuracy of 99%. Another method that applied the convergence of vessels to localize the ONH was proposed by Foracchia et al. [171]. Youssif et al. [172] applied matching the expected directional structure of the vessels for ONH detection. Their method started by normalizing luminosity and contrast

throughout the image using illumination equalization and adaptive histogram equalization methods respectively. Lu and Lim [173] utilized a different approach to place the ONH based on its bright appearance in color retinal image. They used a series of concentric lines with various directions and assessed the image variation along the different directions. Figure 3 shows the retinal images of these categories and related signs.

### 3.1.2. Segmentation of Optic Nerve Head

In case of segmentation methods category, the brightness was applied by Li and Chutatape [174, 175] to detect the ONH candidates for their model-based technique.

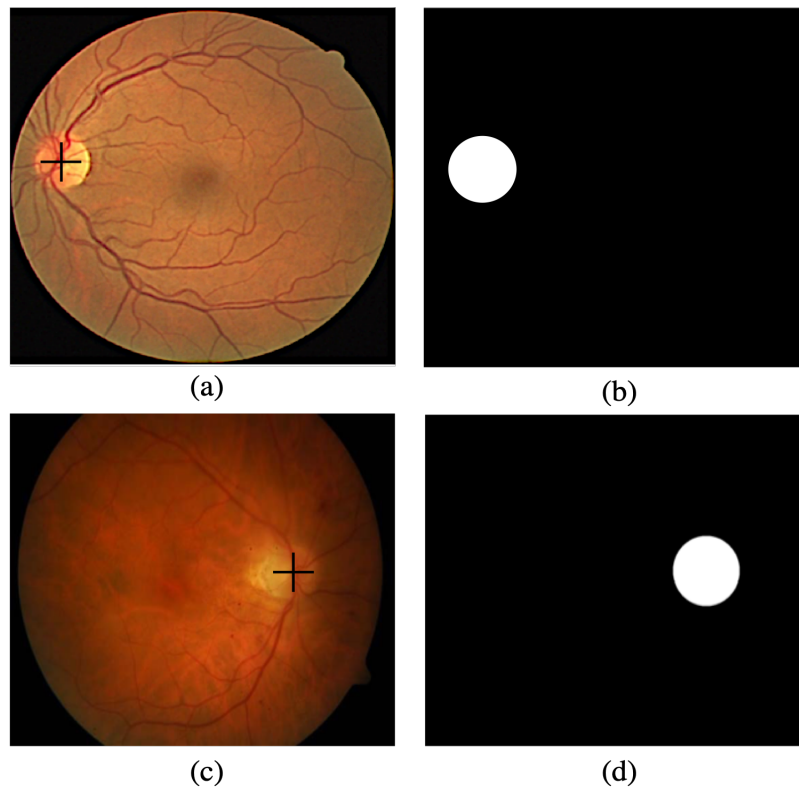


Figure 3: **ONH detection.** (a, c) Retinal images from MUMS-DB and detected center of the ONH; (b, d) ONH mask segmentation.

They established an active shape model, which consisted of building a model with training cases and iteratively matching the landmark points on the disc edges and main vessels inside the disc [170]. A model-based approach was introduced effectively based on active contour model by Osareh et al. [176, 177] to approximately detect the ONH. Lowell et al. carefully created an ONH template, which was then correlated to the intensity component of the retinal image using the full Pearson-R correlation [87]. Another model-based algorithm was introduced by Xu et al. [178]. They applied the deformable contour model technique that included ONH margin. Their method

used a clustering-based classification of contour points and customized contour evolution step integrated in original snake formulation. The approach introduced by Wong et al. [179] was based on the level-set method followed by ellipse matching to smooth the boundary of the ONH. They proposed: 1) the ONH location according to the previously obtained location by means of histogram analysis and initial contour definition, and 2) subsequently, a modified version of the conventional levelset method was used for ONH boundary extraction from the red channel. This contour was finally matched by an ellipse.

On the other hand, Lu [86] introduced a circular transformation to take ONH and its boundary simultaneously. Lalonde et al. presented Hausdorff-based template matching together with pyramidal decomposition and confidence assignment [180]. Pyramidal decomposition acts mainly for detection of large areas with bright pixels, which probable existence of the ONH, but it can be disturbed by large areas of bright pixels that may be near the images borders due to non-uniform illumination. In order to solve this problem, Frank ter Haar [181] used illumination equalization in the green channel of the image, and then a resolution pyramid using a simple Haar-based discrete wavelet transform was formed. Besides, he applied the Hough transform and proposed two methods using a vascular branch constructed from a binary vessel image. Last technique of Frank ter Haar was based on fitting the vessel orientations on a directional model [181]. The ONH identification methods not only apply the characteristics of the ONH, but also extract the location and orientation of vessels [182, 183, 184, 185]. Niemeijer et al. [185] presented the use of local vessel geometry and image intensity features to find the correct positions in the image. A kNN regressor was used to accomplish the integration. Tobin et al. [182] used an algorithm that highly depended on vessel-related the ONH characteristics. They applied a Bayesian classifier to categorized each pixel in images as with/without ONH. Abramoff and Niemeijer [186] applied same properties for the ONH detection, and then a kNN regression was used to estimate the ONH location. The approach developed by Abramoff et al. [187] according to a pixel classification using the feature analysis and nearest neighbor technique. The final results of their algorithm came with the categorization of pixels to a group that belonged to the ONH and non-ONH. In a recent study, Hsiao et al. placed ONH by illumination correction operation, and contour segmentation that was completed by a supervised gradient vector flow snake [188]. To identify ONH location candidates, first template matching was used by Yu et al. Next, they applied vessel features on the ONH to place the location of it. They combined region and local gradient information to the segmentation of the ONH boundary and used Morphological filtering to remove retinal vessels [189].

Moreover, some approaches made use of the fact that all major vessels diverge from the ONH [171, 172, 181, 190]. Most of the studies identified the ONH respect to its shape and color. Other algorithms recognized the ONH according to tracking vessels toward their origin.

Table 5: Summarize of some methods and their results of ONH detection

Authors	ONH detection method	DRIVE	STARE
Sinthabayothin <i>et al.</i> [163]	Highest average variation	99.1%	42%
Walter and Klein [164]	Largest brightest connected object	100%	58%
Li and chutatape [174,175]	Brightness guided, model base	99%	-
Osareh <i>et al.</i> [176,177]	Averaged ONH model based	100%	58%
Lowell <i>et al.</i> [87]	ONH Laplacian of Gaussian template	99%	-
Lalonde <i>et al.</i> [157]	Hausdorff based with pyramidal decomposition and confidence assignment	100%	71.6%
Frank ter Haar [181]	Resolution pyramid using Haar based wavelet transform	89%	70.4%
Frank ter Haar [181]	Hough used only to pixels on or close to the retinal vasculature	96.3%	71.6%
Frank ter Haar [181]	Pyramidal decomposition of both the vascular and green plan	93.2%	54.3%
Frank ter Haar [181]	Hough and fuzzy convergence	97.4%	65.4%
Tobin <i>et al.</i> [182]	Vasculature related ONH features and a Bayesian classifier	81%	-
Abramoff & Niemeijer [185,186]	Vasculature related ONH properties and a kNN regression	99.9%	-
Youssif <i>et al.</i> [172]	matching the expected directional pattern of the retinal blood vessels	100%	98.8%
Hsiao <i>et al.</i> [188]	illumination correction, and contour segmentation is completed by a supervised gradient vector flow snake	100%	90%
Tavakoli <i>et al.</i> [165,168]	Different vessel segmentation methods	90%	85%
Pourreza <i>et al.</i> [53]	Radon Transform	100%	94%

### 3.2. Vessel Segmentation

There is a substantial effort reported in the state of art for the segmentation of retinal vessels in fundus images [56, 91, 94, 95, 97, 191-196]. Overall, the vessel segmentation approaches are

classified in to five categories: *tracking, mathematical morphology, matching filter, model-based thresholding, and supervised classification algorithms* [1]. Table 6 summarizes all these methods and below, we briefly are discussed below.

Table 6: Some vessel segmentation methods

Authors	Method	Classifier &Databases	Evaluation
Xu and Luo [92]	Sobel filter for ONH, Adaptive threshold	Thick & thin vessels, SVM, DRIVE	Acc.= 93.36% Sen. = 85.57%
Hassan et al. [197]	Hidden Markov Model	Vessels, DRIVE	Acc.= 95.7% Sen.= 81.0% Sp. = 97.0%
Dash and Bhoi [89]	Binary difference and enhanced image	DERIVE, CHASEDB1	Acc.= 95.5%,
Nguyen et al. [93]	Linear combination of line responses	SVM, STARE, DRIVE, REVIEW	Acc.= 93.24%, 94.07%,
Fraz et al. [56, 95]	Mathematical morphology, aggregation	DRIVE, STARE MESSIDOR	Acc.= 95.52% Sp. = 97.23%
Marin et al. [96]	Grey level features	ANN, DRIVE, STARE	Acc.= 95.26%, Sen.= 69.44 %sp.= 98.19%
Aslani and Sarnel [198]	Hybrid features	DRIVE, STARE	Acc.= 95.13%, Sen.= 77.96% sp.=97.17%
Lupascu and Trucco [199]	Ada Boost	Ada Boost classifier, DRIVE	Acc.= 95.69% Sen.= 55.74% sp.= 99.36%
Rodrigues et al. [160]	Histogram analysis, Wavelet hessian based and Gaussian filter,	DRIVE, HRF,	Acc.= 94.65%,
Tavakoli et al. [101]	Radon transform	MUMS-DB	Acc.=90%, Sen.=85%
Zhang et al. [94]	kNN	DRIVE	Acc.= 95.05% Sen.= 78.12% Sp.= 96.62%
Zhu et al. [90]	Vessel profile, Gaussian, Morphology	ELM, DRIVE, RIS	Acc.= 96.07, Sen.= 60.18, Sp.= 98.68%
Neto et al. [91]	Binary morphological reconstruction	DRIVE, STARE	Acc.= 86.16%, 87.87% Sen. = 79.42, 76.96% Sp.= 95.37%, 96.31%
Vega et al. [200]	Lattice NN and dendritic processing	ANN	Acc.= 94.83%, Sen.= 96.71%, Sp.= 70.19%
Waheed et al. [201]	Connected component, Binary threshold,	Localized Fisher Discriminant Analysis, DRIVE, STARE	Acc.= 95.81%, 96.16%,
Zilly et al. [202]	Ada Boost	MESSIDOR, DRISHTIGS	-

A comprehensive review on existing methods in retinal vessel segmentation and available public datasets are presented in [52, 33]. In general, vessel segmentation algorithms can be classified into two broad categories: unsupervised and supervised methods [203]. A comparative survey of these two classes has been presented in [102]. Unsupervised methods can be further classified into techniques based on matched filtering [47, 99], morphological processing [204],

vessel tracking, multi-scale analysis [205, 206], line detectors [93] and modelbased algorithms [98, 207]. Supervised segmentation methods are based on pixel classification such as the k-nearest neighbors (kNN) [49], Gaussian mixture models [107], SVM [208], NN [208], decision trees [195], and AdaBoost [199, 96]. They utilize ground truth data for the classification of vessels, based on given features.

The principle of matched filter detection in unsupervised methods was proposed in [47]. With this technique, the authors used a 2D Gaussian-shaped template in all directions to search for vessel components. The kernel was rotated through a range of angles (usually 8 or 12) to detect vessels with different orientations. The resulting image is thresholded to produce a binary representation of the retinal vasculature. Another matched filtering approach used for retinal vessel segmentation [209]. The application of local thresholding strategies, edge detection, matched-filtering and region growing was developed in [209]. Chakraborti et al. [99] applied an unsupervised segmentation approach that combined a "vesselness" filter and matched filter using an orientation histogram. Vermeer et al. [98] achieved vessel detection by thresholding, after convolving the image with a 2D Laplacian kernel. A general framework of adaptive local thresholding based on combination of applying a multithreshold scheme and classification procedure to prove all binary result objects were applied by Jiang et al. [210]. Zana et al. [106] proposed a morphology-based approach using an algorithm that combined morphological filters and cross-curvature evaluation to segment vessel-like patterns in retinal images. Other mathematical morphology approaches are described in [204, 105, 211]. Heneghan et al. [211] combined morphological transformations with curvature information and matched filtering for centerline detection. In [100] vessels are extracted using multiple structure elements followed by connected component analysis. Martinez-Perez et al. [205] introduced an automated algorithm for retinal images based on a multi-scale feature detection. The local maxima of the gradient magnitude and the maximum principal curvature of the Hessian tensor were used in a multi-pass region growing process. This procedure accurately segmented the retinal vasculatures by using both feature and spatial information. Zhang et al. [206] employed innovative rotating multi-scale second-order Gaussian derivative filters which are referred to as orientation scores for the enhancement and segmentation of blood vessels. Roychowdhury et al. proposed an iterative unsupervised retinal vessel segmentation algorithm that used an adaptive threshold and a region growing method with a stopping criterion to terminate the iteration [212].

Nguyen et al. proposed a vessel detection method based on line detection [93]. This approach was based on this fact that changing the length of a line detector makes line detectors with variety of scales. The final vessel segmentation results were achieved by combining line responses at varying scales. The combination of shifted filter responses for detection of bar-shaped structures in retinal images was presented by Azzopardi et al. [104]. Their approach was rotation invariant,

where the selection of the orientations was chosen from given the structures similar to vessels which suffered from difficult crossing cases. Lam and Yan [207] used the Laplacian operator to segment blood vessels and detect centerlines from the normalized gradient vector field, pruning noisy objects. Vessel continuity employs measures of width and orientation, iteratively calculated in a local region near the current point, in order to track along the length of a vessel [100, 103]. Tavakoli et al. [101] presented the combination of Radon transformation and multi-overlapping windows to segment the retinal vessels. Since their approach relied on the concept of Radon, which is integral based, they suppressed the intrinsic noise of images by using this transformation.

Supervised approaches use a pixel classification method, referred to as a primitive-based approach by Staal et al. [213]. This approach was based on the detection of ridges, used as primitives for introducing linear segments, called line elements. Sinthanayothin et al. [163] identified retinal vessels using a NN whose inputs were deduced from PCA of the image and edge extraction of the first principal component. A NN and backpropagation multilayer method was proposed by Gardner et al. [123] for vessel tree detection following histogram equalization. The kNN classifier was implemented by Niemeijer et al. [49]. In their algorithm, from the green plane of the RGB image, a vector of 31-component pixel feature was created with the Gaussian and its derivatives up to order 2 at 5 different scales. Soares et al. [107] applied a Gaussian mixture model Bayesian classifier. By using the Gabor wavelet transform, multiscale analysis was performed on the image. Ricci and Perfetti [208] utilized a SVM for classifying pixels as vessel or non-vessel. In their algorithm, along with the gray-level of the target pixel they applied two orthogonal line detectors to create the feature vector. One of the interesting supervised methods was implemented by Fraz et al. [56] which was an ensemble classification system of boosted and bagged decision trees. The drawback of supervised classifications is its necessity for a sufficient number of manually annotated training image set. Moreover, they are not easy to generalize the trained models to meet the needs of different datasets. More recent studies have successfully applied the concept of deep learning to the segmentation of the retinal vasculature [90, 214-223].

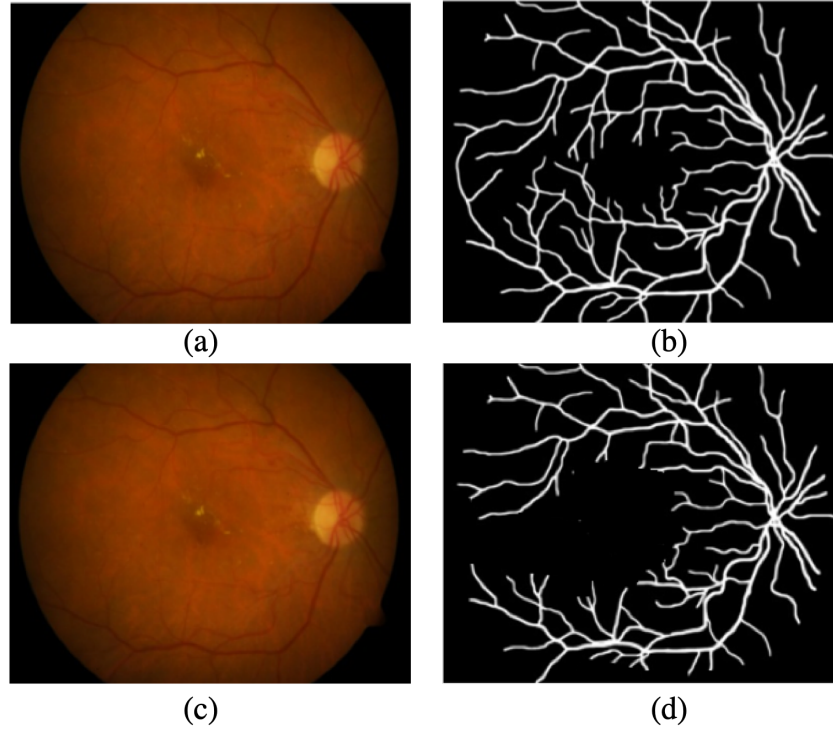


Figure 4: **Vessel segmentation.** (a, c) Retinal images from MUMS-DB; (b, d) Vessel segmentation results.

### 3.3. Localization of the Fovea

Fovea is small region approximately at the center of retina and responsible for central and high resolution vision. It is placed around 45 times of ONH radius to the temporal direction of ONH [163, 170, 185, 224, 225, 226, 152, 227, 228, 229]. The visual cells placed in the fovea are closely packed and cause the highest sharpness of vision [230]. No blood vessels passing through the fovea to obstruct the crossing of light considerable the foveal cells [231]. The fovea detection approaches are divided in to two classes: hybrid and constraints based approaches [1].

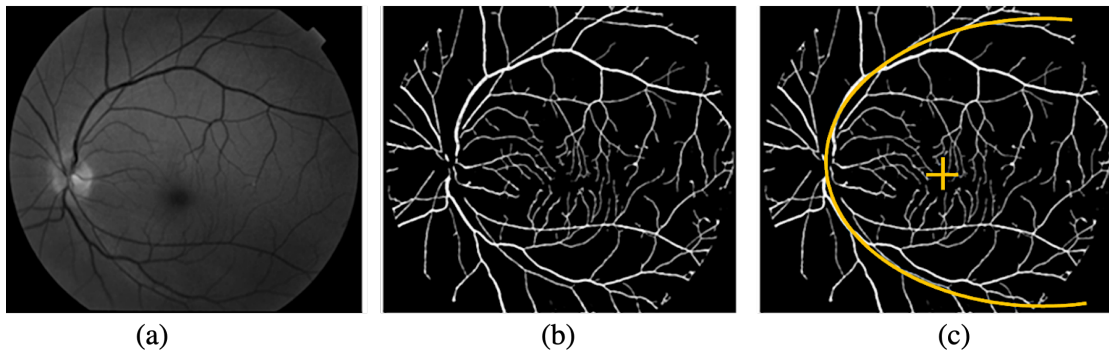


Figure 5: **Fovea detection.** (a) Retinal images from MUMS-DB; (b) Vessel segmentation results; (c) Detected fovea.

### 3.3.1. Hybrid-based method

Sinthanayothin et al. [163] presented a method for fovea localization using intensity correlation. At the beginning, fovea was behaved with intensity correlation and from HSI transformation the peak was selected. The selected peak located a dark area and was considered as fovea. The disadvantageous of their method was when the fovea was not at the center it failed. In another method, using location of fovea, a polar retina coordinate system was established. Here, the fovea accurately was located using its appearance and geometry according to other landmarks [170]. Niemeijer et al. [185] proposed a method to identify the fovea based on single point distribution model. The method included all signs including global and regional, to identify this model. These signs were extracted from the related vessel position and its width. Tavakoli et al. [148] proposed an approach based on vessel segmentation and parabola fitting to identify the fovea. Their algorithm was included of 4 steps: multi-overlapping windows, local Radon transform, vessel validation, and parabolic fitting.

### 3.3.2. Positional constraints-based

The positional restrictions ( [163, 170, 184, 185, 224, 225, 226]) were applied to localize the fovea and determine its position. The fovea identification was obtained using the location of other retinal regions. The main part of this approach [182] specifies the horizontal retinal ridge that is passing across the ONH and fovea, which divides the upper and lower retinal regions. Further, the region of fovea was extracted using fixed distance of 5 ONH radius from the ONH center.

Table 7: Details of some of fovea detection methods.

Author	Approach	No. of images	Accuracy
Sinthabayothin et al. [163]	NN and template-based	112	80.4%
Li and Chutatape [175]	Modified active shape model	35	100%
Tavakoli et al. [148]	Fitting the main vessels with parabola function	140	90%
Tobin et al. [182]	ONH and fovea localization	345	92.5%
Seckar et al. [232]	Hough transform and morphological function	44	100%
Fleming et al. [184]	Vessel segmentation with semiellipse fitting	1056	96.6%
Niemeijer et al. [185]	Point distribution model and kNN	500	96.8%

Welfer et al. [233]	ROI Sselection and morphological operator	126	96.1%
---------------------	---	-----	-------

#### 4. Detection of retinal lesions

An acceptable CAD system requires to identify lesions such as MAs, HEs, EXs, CWS, and NVs as perfect as possible to finally result in distinguishing between DR and no DR image. Several studies have been worked on various detection and segmentation approaches to detect these lesions. Here, we briefly have discussed them.

##### 4.1. Microaneurysms and Haemorrhages Detection:

The most reliable method for MA detection is from fluorescein angiography retinal images [19]. However, the fluorescein angiography images are costly, invasive and not suitable for everyone [22]. Moreover, this approach is time-consuming. Introductory global image processing approaches were applied for automated detection. There are a number of methods for the detection of both MAs and HEs. These methods can be generally categorized into two general groups including unsupervised and supervised approaches [17, 22, 108, 109, 111, 112, 227, 234-248]. Many studies have searched both MAs and HEs detection from the retinal images by suing proper thresholding after masking the landmarks such as ONH, fovea, and vessel. After the thresholding, mathematical morphology was used to distinguish MAs and other structures, such as bifurcations and small vessels. From unsupervised viewpoint, the MAs detection approaches are classified in to different classes: morphology, region growing, wavelet, and hybrid approaches [1]. Among these groups, the HEs detection is mostly based on mathematical morphology combine with pixel classification. In this section, we briefly explain the related studies.

Walter et al. [22] presented a 4-part method for MAs detection. At the beginning, the preprocessing step used green channel images. The top-hat transformation and global thresholding were used to identify MAs. Next, fifteen characteristics were used to differentiate true MAs from false ones using kNN, Gaussian and kernel density classifiers. Hatanaka et al. [249] proposed a brightness correction approach for automated detection of HEs. The correction was applied in Hue Saturation Value (HSV) space.

In the morphological approach, different adjustments often increase the accuracy of MAs detection [17, 241]. In spite of this type of hand-crafted method, typically is fast, easy, and user friendly but the ability of it is constrained by its builder. In better words, some main hidden structures and uncovered patterns might be ignored by the builder and cause false detection [111]. The morphological operations such as closing [22], or using top-hat transformation [19] has been applied for MAs detection due to their relatively uniform circular shape and limited size range.

However, besides the above issue, most of the mathematical morphology methods mainly depend on the choosing of optimal structuring elements; changing their size and shape decreases the efficiency of these algorithms.

Fleming et al. [17] developed contrast normalization, watershed and region growing approaches to detect MAs in retinal images. Moreover, they applied a 2D Gaussian-aftermedian filtering to preprocess the image. To detect MAs they used the kNN classification using nine characteristics from extracted candidates. Sinthanayothin et al. [21] identified MAs by applying region growing and adaptive intensity thresholding, combined with a moat operator. Quellec et al. [108] used wavelet transform algorithm for MAs detection by matching wavelet sub-bands with the lesion template.

Tavakoli et al. [19] employed an approach based on top-hat, mathematical morphology and Radon transform, applied locally in multi-overlapping windows to detect MAs. Niemeijer et al. [234] introduced a hybrid red lesion detection method using ideas from Spencer et al. [250] and Frame et al. [251]. At the beginning, using pixel classification the red lesion candidates were identified [250]. The MAs and HEs were detected after masking the vessels. Usher et al. [132] and Gardner et al. [123] applied NN to locate MAs. Initially, they used local adaptive contrast enhancement to preprocess the image. After that landmarks (ONH and vessel segmentation), and red lesions (MAs and HEs) were identified using region growing and adaptive intensity thresholding combined with moat operation [21]. Zhang et al. [252] described a method using Multi-Scale Correlation Filtering and threshold values within angiographic retinal image for MA detection. They used a moving Gaussian kernels to extract the correlation coefficient for pixels. Larsen et al. [146] introduced an automatic MAs and HEs detection approach using classification algorithm called RetinaLyze using shape and size of the lesions.

Fleming et al. [133] applied multiscale and morphological operators to place HEs. For the preprocessing, they corrected the variations in intensity and contrast by applying median filter and histogram equalization. In another study [17], they proposed a region growing algorithm to identify large lesion regions. In their approach, they had difficulty differentiating HEs and MAs. Zhang and Chutatape [253] introduced an approach to detect HEs using SVM. In addition, they applied PCA to detect the features. These features were used as the inputs of SVM to extract HEs. Hipwell et al. [254] proposed an automated MA detection in red-free retinal images. To remove variation in the illumination, a shading correction was applied to the image.

Another approach in contrast with linear landmarks like vessels, which are directional, is to utilize template matching filters with multiscale Gaussian kernels [108, 252, 236]. According to statistical results, the intensity distribution of MAs is matched to a Gaussian distribution [108] because MAs display Gaussian profiles in all projections. Therefore, template matching filter

highly increased the accuracy of MA detection. Using this idea, Quellec et al. proposed a wavelet transform method for MA detection. In their algorithm, they detected the MAs using a local template matching filter in the wavelet domain [108]. Zhang et al. [252] used a multi-scale correlation coefficient based approach. In their method, they used a nonlinear filter with five Gaussian kernels at various standard deviations to detect MA candidates. Ram et al. [240] described a feature based method that rejects specific classes of clutter while accepting a higher number of true MAs. The potential MAs, obtained after the final step, are labeled a grade that was based on their shape similarity to true MAs. Same as the morphological approach, this type of algorithms is still limited by ignorance of hidden and unnoticeable structures. Moreover, a lot of parameters required to be assigned empirically.

The brief explanation of the MAs and HEs detection algorithms is introduced in Table 8.

Table 8: Details of some of MA and HE detection methods

Authors	Methods	Performance
<b>MA detection</b>		
Tavakoli et al. (2013) [19]	Radon transform	Sen. = 92%, Sp. = 90%
Hipwell et al.(2000) [254]	Matched filter, region growing	Sen. =81%, Sp. = 93%
Sinthanayothin et al. (2002) [21]	Moat operator	Sen. =77.50%, Sp. = 88.70%
Larsen et al. (2003) [146]	Size and shape	Sen. =71.4%
Usher et al. (2004) [132]	Moat operator	Sen. =95.10%, Sp. = 46.30%
Niemeijer (2005) [234]	Pixel classification using kNN	Sen. =100%, Sp. = 87%
Fleming et al. (2006) [17]	Contrast normalization, watershed region growing	Sen. =85.40%, Sp. = 83.10%
Walter et al. (2007) [22]	Gaussian filtering, top-hat	Sen. =88.5%
Quellec et al. (2008) [108]	Optimal wavelet transform	Sen. = 89.62%, Sp. = 89.50%
Zhang et al. (2010) [252]	Multi-scale correlation filtering and dynamic thresholding	Sen. =71.30%
Sanchez (2011) [73]		Sen. =91%
Antal and Hajdu (2012) [255]	Ensemble-based	AUC=0.90
Lazar and Hajdu (2013) [236]	Cross section features	-
Pereira (2014) [113]	multi-agent system approach	Sen. = 87%
Seoud (2016) [23]	Dynamic Shape Features	Sen. = 84.4%
Srivastava (2017) [110]	Filters for feature extraction	-
<b>HE detection</b>		
Gardner (1996) [123]	NN and Statistical threshold tuning	Sen. = 73.80%
Zhang and Chutatape (2005) [253]	PCA and SVM	Sen. = 89.10%
Fleming et al. (2008) [133]	Multi-scale, morphology and SVM	Sen. = 98.60%, Sp. = 95.50%
Hatanaka et al. (2008) [249]	Brightness correction and thresholding	Sen. = 80%, Sp. = 88%

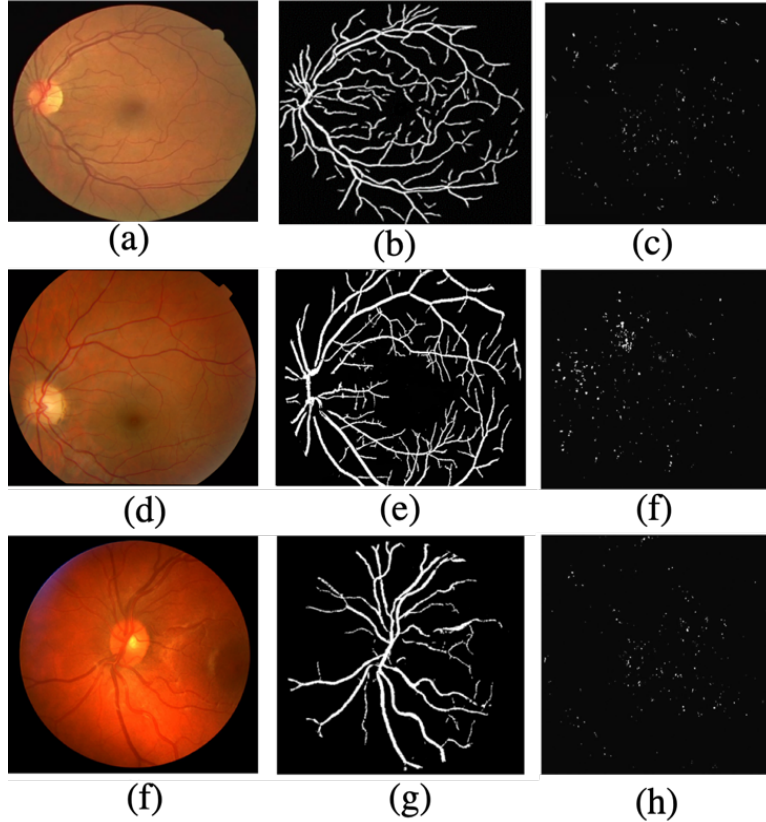


Figure 6: **MA detection.** (a, d, f) Retinal images from different datasets; (b, e, g) Vessel segmentation and masking results; (c, f, h) Detected MAs.

#### 4.2. Exudates Segmentation

Here, we briefly review the studies of EXs segmentation. EXs are one of the main signs of DR, because they cause retinal edema and consequently vision loss and blindness. The approaches for identification of EXs [256, 257, 258, 114] can be categorized into four classes: pixel clustering, morphology, thresholding/region growing, and classification-based approaches [1]. Here, we concisely introduce these methods.

Several studies [120, 259, 260] have used Fuzzy C-Means cluster-based method for EXs detection. This method suggests pixels with various classes and changing degrees of membership for segmentation purpose [261, 262]. Osareh et al. [259] first by correcting color and contrast worked on image preprocessing. The preprocessed images were used for segmentation step using Fuzzy C-Means. The genetic algorithm was applied to choose characteristics from Fuzzy C-Means clustered regions [260]. The optimal characteristics were then used in the NN to detect EXs and non-EXs regions. This approach cops the differing retinal color. In another study, the EXs were segmented from low quality images using Fuzzy C-Means [120]. The same authors presented EXs detection using Bayesian classifier [120]. Hsu et al. [69] described an algorithm of EXs

segmentation using cluster-based approach. Then, cluster-based method was utilized to classify the abnormal pixels. The restrictions of the above methods is to know considerable clusters which contribute to the EXs detection.

Morphological [263, 264, 121] and thresholding/region growing methods [21, 136] were applied in many studies about EXs detection. Sopharak et al. [263] presented an EXs segmentation approach for low image quality by applying adjusted morphology. Walter et al. [264] detected EXs using gray level changes of green channel. After first step detection, their boundaries were determined applying a morphological reconstruction approach. Their method did not differentiate EXs from CWS. Sanchez et al. [121] used same approach as Walter et al. [264] used in preprocessed the green channel and histogram of the image was modelled using a Gaussian Mixture Model. Furthermore, a thresholding method was utilized to detect the EXs using Gaussian Mixture Model. Sinthanayothin et al. [21] developed a region growing-based method by selecting some threshold values in the gray scale images. To improve the quality of image, adaptive local contrast enhancement was applied. This algorithm located other retinal regions and landmarks such as the ONH, retinal vessels and fovea. Fleming et al. [184] presented a multi-scale morphology algorithm to localize EXs. They used Gaussian and median filter to preprocess the green channel images for correcting the contrast variations. A watershed region growing algorithm was used to separate the EXs from other landmarks. Finally, They used SVM to classify regions into EXs and non-EXs. Welfer et al. [265] presented an EXs detection algorithm based on Morphology operator. They applied a set of morphological functions to detect EXs. Mookiah et al. [136] introduced EXs detection by applying color, shape and morphological processing. Their method assumed EXs to have higher contrast than the ONH.

Several studies [123, 234, 266] utilized machine learning approaches to categorize EXs and non-EXs pixels. Gardner et al. [123] utilized NN to classify EXs applying gray scale of retinal images. Sanchez et al. [266] segmented EXs according to Fishers Linear Discriminant Analysis. They used color normalization and contrast enhancement. Niemeijer et al. [234] introduced an automated method for EXs detection using classification based on machine learning idea. The pixels with high probability were classified into EX class from non-EXs.

## **5. Artificial Intelligence in Diabetic Retinopathy**

In general, understanding and controlling DR or other retinal diseases has become extensively more complicated because of the large number of images and diagnoses. In fact, processing all these patient examinations seems as a big data challenge [267]. Clearly, the new era of diagnosis and clinical data mining immediately needs intelligent systems to control them sufficiently, safely and efficiently.

Recently, through the advancement of supervised learning ideas, the recent application of artificial intelligence (AI) approaches for DR detection and its related lesions have significantly increased in the research community. AI has already revealed proof-of-concept in medical science such as radiology and pathology, which like ophthalmology relies heavily on diagnostic imaging. As it turns out, image processing is the most important application of AI in healthcare [268]. Moreover, AI is particularly suitable in assisting clinical tasks by using efficient algorithms to identify and learn features from large volumes of imaging data, and helping to reduce diagnostic errors. In addition, it can recognize specific patterns or lesions and correlate novel characteristics to obtain innovative scientific insight [269].

The most important branch of AI is machine learning (ML) [269] where the rules would be learned directly by algorithms from a series of examples, called training data, instead of being encoded by hand. ML techniques need that a set of biomarkers or characteristics to be measured directly from the training data (e.g., labeled lesions in retinal image). After that based on a training database of characteristics with known labels, i.e. hand crafted features, a classifier learns to identify the correct label from the newly seen characteristics. Once a few strong classifiers have been established, the effectiveness of such ML models mostly relies on the differentiative power of the chosen characteristics which underpin the classifier performance. There are different reviews that have summarized ML approaches [1, 15, 74, 270-273]. Both Mookiah et al. [1] and Mansour [74] classified DR diagnosis methods in respect to affiliated methods, such as DR lesion tracking, mathematical morphology, cluster-based, matched filter, and hybrid methods. Faust et al. [15] surveyed studies that detect lesion characteristics from retinal images, such as the retinal vessels, MAs, HEs, and EXs. Joshi and Karule [270] summarized the first researches on EXs segmentation. Almotiri et al. [271] came up with a survey of methods to detect the vessels. Almazroa et al. [272] and Thakur and Juneja [273] studied several approaches for ONH detection.

Recently, the accessibility of large databases and the immense computing power suggested by advanced graphics processing units have research on Deep Learning (DL) based methods, which have demonstrated magnificent efficiency in all medical sciences. Many DL-based approaches have been established for variety of works to analyze images to establish automated CAD systems for detection of DR. The relation between AL, ML, and DL has been shown in the figure below:

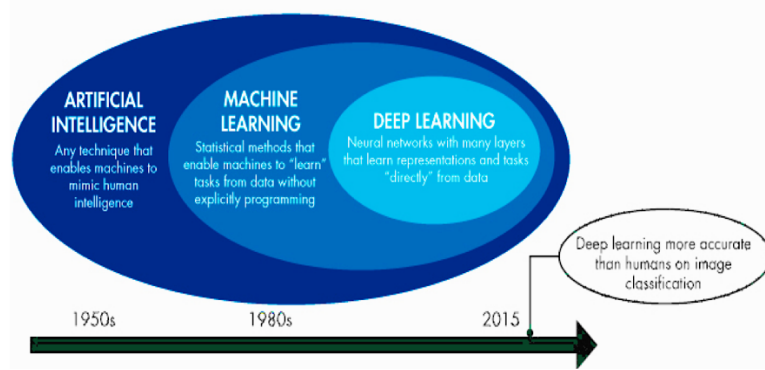


Figure 7: **AI, ML, and DL.** Relation between artificial intelligence, machine learning and deep learning.

### 5.1. Overview of Deep Learning

There are multiple DL-based algorithm that have been presented. Some frequently utilized deep architectures for the DR detection purpose include convolutional neural networks (CNNs), autoencoders (AEs), recurrent neural networks (RNNs) and deep belief networks (DBNs). A complete overview of these architectures is found in [274]. There are several DL-based architectures related to DR detection [275-285]. Based on the clinical significance of automated DR detection, we group application of DL into three broad classes: (i) vessels segmentation, (ii) ONH localization and segmentation, and (iii) retinal lesions detection and classification. In the below sub-sections, we briefly introduce the literatures about DL-based algorithms for these tasks. The brief summary of the DL methods in DR detection systems is presented in Table 9.

#### 5.1.1. Retinal Blood Vessel Segmentation

Many of the retinal vessel segmentation approaches are based on CNN architectures [217, 218, 286-290].

Maji et al. [286] proposed 12 CNN models for this purpose. Each CNN model included three convolutional layers and two fully connected layers. Liskowski and Krawiec [218] introduced a supervised pixel-wise algorithm using deep CNN, which was trained by preprocessed retinal images, and augmented using geometric transformations. Tan et al. [217] employed a 7-layer CNN model to segment blood vessels, ONH, and fovea.

Some methods use AEs in segmentation of retinal vessels [291, 292]. Roy and Sheet [291] presented an AE-based deep NN model that used the domain adaptation method for training the model. AE-based deep NN included of two hidden layers, which were trained using the source domain databases, using an autoencoding and supervised mechanism. The algorithm introduced by Maji et al. [286] employed a hybrid DL, which consisted of unsupervised stacked denoising AEs with total 500 layers, to segment vessels in retinal images.

### 5.1.2. *Optic Nerve Head Detection*

As we mentioned at the beginning of this chapter, ONH identification can improve DR detection and classification. In fact, the ONH brightness can cause uncertainty for detecting of other bright lesions such as EXs. There are number of studies that work on both ONH detection and segmentation using concept of DL [202, 293-296].

Lim et al. [293] presented a nine-layer CNN model for ONH segmentation. Their algorithm involved different steps: detecting the region around the ONH, enhancement, classification at pixel-level using a CNN model to predict the ONH. Tan et al. [217] identified the ONH and vessels jointly using pixel patch-based CNN. Zilly et al. [202] presented an ONH segmentation algorithm based on a multiscale two-layer CNN model. At first, the area around the ONH was cropped, and down-sampled. After that, the area was analyzed by entropy filtering to determine the most distinguished points and was passed to the CNN model for final segmentation. Zhang et al. [294] applied a faster CNN to localize the ONH. After identifying the ONH, the thick vessels inside its area were eliminated by using a Hessian matrix, and its boundaries segmented.

### 5.1.3. *Microaneurysms and Hemorrhages detection*

Many DL-based approaches have been introduced for detection and classification of different types of DR lesions such as MAs, and HEs [2, 6, 16, 112, 115, 275, 276, 297-301].

Halo [297] introduced a nine-layer CNN model to group each pixel as MA or non-MA and grading the DR. Each pixel is categorized by taking a window around the candidate and passing it to the CNN model. For training, they applied a data augmentation method to create six windows around each pixel. van Grinsven et al. [112] worked on detecting HEs. Their main contribution of was to overcome the over-represented normal samples created for training a CNN model. To figure out this issue, they employed a dynamic selective sampling idea that selects informative training samples. Their CNN was trained using a dynamic selective sampling strategy as well.

Gondal et al. [302] and Quellec et al. [277] also detected HEs and small red dots. Another similar approach was introduced by Orlando et al. [106]. In their approach, they first extracted red candidates using morphological operations. Next, they extracted CNN and hand-engineered characteristics such as intensity and shape from each candidate to introduce a probability map, which was utilized to make both red lesion and image level decision. Shan and Li [299] applied the stacked sparse AEs to identify MAs. A patch was passed to stacked sparse AEs, which extracted characteristics, and the Softmax classifier labeled it as a MA or non-MA patch. Tavakoli et al. employed a CNN approach to detect MAs. In their approach, they first extracted candidates using morphological functions. Next, they used CNN classification to classify between MAs and non-MAs. In their study, the authors compared effect of two preprocessing methods, Illumination

Equalization, and Top-hat transformation, on retinal images to detect MAs using combination of Matching based approach and CNN methods [6].

#### *5.1.4. Exudates Detection*

There are different studies on EX detections using DL [303, 304, 302, 277]. Prentasic and Loncaric [304] employed a CNN-based algorithm for EXs detection in retinal images. First, they detected the ONH, created a probability map for that. Then they created for both vessels and bright-boundary probability maps. At the end, they applied an 11-layer CNN model to produce an EX probability map and finally segment the EXs. Gondal et al. [302] presented an algorithm for EXs detection combine with other DR lesions based on CNN architecture [305]. To identify DR lesions including different types of EXs and HEs, the dense layers were removed from the CNN model. For detecting DR lesions such as EXs at the pixel level, Quellec et al. [277] proposed a CNN visualization methods. The authors did a modification on their CNN based on the sensitivity evaluation done by Simonyan and Zisserman [306], which helped in detecting DR and lesions by optimizing CNN predictions.

*Table 9: Details of some of MA and HE detection methods*

Authors	Methods	Training	Type	Database	Performance
Maji et al. [286]	Patch-based ensemble of CNN	End-to-end	Vessel segmentation	DRIVE	AUC=0.9283 ACC= 94.7
Liskowski and Krawiec [218]	Patch-based CNN	End-to-end	Vessel segmentation	DRIVE, STARE, CHASE	AUC=0.9790, 0.9928, 0.988 ACC=95.35, 97.29, 96.96
Maninis et al. [218]	Fully CNN (FCN)	Transfer learning	Vessel segmentation	DRIVE, STARE	-
Wu et al. [100]	tracking/patch-based CNN/PCA as classifier	End-to-end	Vessel segmentation	DRIVE	AUC=0.9701
Dasgupta and Singh [288]	Patch-based FCN	End-to-end	Vessel segmentation	DRIVE	AUC=0.974 ACC=95.33
Tan et al. [217]	Patch-based CNN	End-to-end	Vessel segmentation	DRIVE, STARE	ACC=94.70, 95.45
Mo and Zhang [290]	Multi-level FCN	End-to-end	Vessel segmentation	DRIVE, STARE, CHASE	AUC=0.9782, 0.9885, 0.9812 ACC=95.21, 96.76, 95.99
Maji et al. [286]	Patch-based AE	Transfer learning	Vessel segmentation	DRIVE	AUC=0.9195, ACC=93.27
Li et al. [292]	Patch-based AE	End-to-end	Vessel segmentation	DRIVE, STARE, CHASE	AUC=0.9738, -, 0.9716, ACC=95.27, 96.28, 95.81
Lahiri et al. [291]	Patch-based AE	Transfer learning	Vessel segmentation	DRIVE	ACC=95.3
Fu et al. [289]	Patch-based CNN as RNN	End-to-end	Vessel segmentation	DRIVE, STARE, CHASE	ACC=95.23, 95.85, 94.89
Lim et al. [293]	CNN with exaggeration	End-to-end	ONH segmentation	MESSIDOR, SEED-DB	-
Tan et al. [217]	CNN	End-to-end	ONH segmentation	DRIVE	ACC=87.90
Sevastopolsky [295]	Modified U-Net CNN	Transfer learning	ONH segmentation	DRION-DB	-
Zilly et al. [202]	Multi-scale CNN	End-to-end	ONH segmentation	DRISHTI-GS	-
Alghamdi et al. [296]	Cascade CNN, each model	End-to-end	ONH detection	DRIVE, DIARETDB1, MESSIDOR, STARE,	ACC=100, 98.88, 99.20, 86.71

Xu et al. [178]	CNN based on deconvolution	Transfer learning	ONH detection	MESSIDOR, STARE	ACC=99.43, 89
Haloi [297]	9-layer CNN	End-to-end	MA detection	MESSIDOR, ROC	AUC=0.982 ACC=95.4
van Grinsven et al. [112]	Patches based selective sampling	End-to-end	HE detection	Kaggle, MESSIDOR	AUC=0.917, 0.979
Gondal et al. [302]	CNN model	Transfer learning	HE detection	DIARETDB1	-
Quellec et al. [277]	CNN model	Transfer learning	HE detection	DIARETDB1	AUC =0.614
Orlando et al. [115]	HEF + CNN and RF classifier	End-to-end	MA-HE detection	DIARETDB1 , e-optha, MESSIDOR	AUC=0.8932
Tavakoli et al. [2,6,16]	Patches CNN	End-to-end	MA detection	DRIVE, DIARETDB1 , MESSIDOR	ACC=95.97
Shan and Li [299]	Patches based AE	Transfer learning	MA detection	DIARETDB	ACC=91.38
Prentasic and Loncaric [304]	11-layer CNN,	End-to-end	EX detection	DRiDB	-
Gondal et al. [302]	CNN model	Transfer learning	EX detection	DIARETDB1	
Quellec et al. [277]	CNN model	Transfer learning	EX detection	DIARETDB1	AUC=0.974,

## 6. Conclusion

This chapter introduces a detailed studies of methods and their results for DR detection and classification using retinal image. The DR is a complication of diabetes that damages the retina, and causes vision loss and blindness. A robust DR screening system will remarkably decrease the workload of clinicians. The screening process brings sets of steps namely identifying and segmenting the retinal landmarks, detecting lesions, feature extraction and classification. All these steps need different methods and techniques. Although considerable accomplishments have been made in digital retinal image analysis, there are variety of challenges in the selection of suitable approaches which result in high accuracy during DR screening.

## References

- [1] Mookiah MRK, Acharya UR, Chua CK, Lim CM, Ng E, Laude A. Computer-aided diagnosis of diabetic retinopathy: A review. *Computers in biology and medicine* 2013;43(12):2136–55.

- [2] Tavakoli M, Jazani S, Nazar M. Automated detection of microaneurysms in color fundus images using deep learning with different preprocessing approaches. In: *Medical Imaging 2020: Imaging Informatics for Healthcare, Research, and Applications*; vol. 11318. International Society for Optics and Photonics; 2020, p. 113180E.
- [3] Thomas RL, Dunstan FD, Luzio SD, Chowdhury SR, North RV, Hale SL, et al. Prevalence of diabetic retinopathy within a national diabetic retinopathy screening service. *British Journal of Ophthalmology* 2015;99(1):64–8.
- [4] Zana F, Klein JC. Segmentation of vessel-like patterns using mathematical morphology and curvature evaluation. *IEEE transactions on image processing* 2001;10(7):1010–9.
- [5] Nayak J, Bhat PS, Acharya R, Lim CM, Kagathi M. Automated identification of diabetic retinopathy stages using digital fundus images. *Journal of medical systems* 2008;32(2):107–15.
- [6] Tavakoli M, Nazar M. Comparison different vessel segmentation methods in automated microaneurysms detection in retinal images using convolutional neural networks. In: *SPIE*; vol. 11317. 2020, p. 113171P.
- [7] Cade WT. Diabetes-related microvascular and macrovascular diseases in the physical therapy setting. *Physical therapy* 2008;88(11):1322–35.
- [8] Emdin CA, Rahimi K, Neal B, Callender T, Perkovic V, Patel A. Blood pressure lowering in type 2 diabetes: a systematic review and meta-analysis. *Jama* 2015;313(6):603–15.
- [9] Schaffer SW, Jong CJ, Mozaffari M. Role of oxidative stress in diabetes-mediated vascular dysfunction: unifying hypothesis of diabetes revisited. *Vascular pharmacology* 2012;57(5-6):139–49.
- [10] Patz A. Studies on retinal neovascularization. Friedenwald lecture. *Investigative ophthalmology & visual science* 1980;19(10):1133–8.
- [11] Niemeijer M, van Ginneken B, Russell SR, Suttorp-Schulten MS, Abramoff MD. Automated detection and differentiation of drusen, exudates, and cotton-wool spots in digital color fundus photographs for diabetic retinopathy diagnosis. *Investigative ophthalmology & visual science* 2007;48(5):2260–7.

- [12] Tavakoli M, Mehdizadeh A, Pourreza R, Banaee T, Bahreyni Toossi MH, Pourreza HR. Early detection of diabetic retinopathy in fluorescent angiography retinal images using image processing methods. *Iranian Journal of Medical Physics* 2010;7(4):7–14.
- [13] Antonetti DA, Barber AJ, Bronson SK, Freeman WM, Gardner TW, Jefferson LS, et al. Diabetic retinopathy: seeing beyond glucose-induced microvascular disease. *Diabetes* 2006;55(9):2401–11.
- [14] Watkins PJ. Retinopathy. *Bmj* 2003;326(7395):924–6.
- [15] Faust O, Acharya R, Ng EYK, Ng KH, Suri JS. Algorithms for the automated detection of diabetic retinopathy using digital fundus images: a review. *Journal of medical systems* 2012;36(1):145–57.
- [16] Tavakoli M, Nazar M, Mehdizadeh A. The efficacy of microaneurysms detection with and without vessel segmentation in color retinal images. In: *Medical Imaging 2020: Computer-Aided Diagnosis*; vol. 11314. International Society for Optics and Photonics; 2020, p. 113143Y.
- [17] Fleming AD, Philip S, Goatman KA, Olson JA, Sharp PF. Automated assessment of diabetic retinal image quality based on clarity and field definition. *Investigative ophthalmology & visual science* 2006;47(3):1120–5.
- [18] Pourreza HR, Bahreyni Toossi MH, Mehdizadeh A, Pourreza R, Tavakoli M. Automatic detection of microaneurysms in color fundus images using a local radon transform method. *Iranian Journal of Medical Physics* 2009;6(1):13–20.
- [19] Tavakoli M, Shahri RP, Pourreza H, Mehdizadeh A, Banaee T, Toosi MHB. A complementary method for automated detection of microaneurysms in fluorescein angiography fundus images to assess diabetic retinopathy. *Pattern Recognition* 2013;46(10):2740– 53.
- [20] Tavakoli M, Naji M, Abdollahi A, Kalantari F. Attenuation correction in spect images using attenuation map estimation with its emission data. In: *Medical Imaging 2017: Physics of Medical Imaging*; vol. 10132. International Society for Optics and Photonics; 2017, p. 101324Z.

- [21] Sinthanayothin C, Boyce JF, Williamson TH, Cook HL, Mensah E, Lal S, et al. Automated detection of diabetic retinopathy on digital fundus images. *Diabetic medicine* 2002;19(2):105–12.
- [22] Walter T, Massin P, Erginay A, Ordonez R, Jeulin C, Klein JC. Automatic detection of microaneurysms in color fundus images. *Medical image analysis* 2007;11(6):555–66.
- [23] Seoud L, Hurtut T, Chelbi J, Cheriet F, Langlois JP. Red lesion detection using dynamic shape features for diabetic retinopathy screening. *IEEE transactions on medical imaging* 2015;35(4):1116–26.
- [24] Group ETDRSR, et al. Grading diabetic retinopathy from stereoscopic color fundus photographs—an extension of the modified airlie house classification: Etdrs report number 10. *Ophthalmology* 1991;98(5):786–806.
- [25] Cusick M, Chew EY, Chan CC, Kruth HS, Murphy RP, Ferris III FL. Histopathology and regression of retinal hard exudates in diabetic retinopathy after reduction of elevated serum lipid levels. *Ophthalmology* 2003;110(11):2126–33.
- [26] McLeod D. Why cotton wool spots should not be regarded as retinal nerve fibre layer infarcts. *British Journal of Ophthalmology* 2005;89(2):229–37.
- [27] Chui TY, Thibos LN, Bradley A, Burns SA. The mechanisms of vision loss associated with a cotton wool spot. *Vision research* 2009;49(23):2826–34.
- [28] Vallabha D, Dorairaj R, Namuduri K, Thompson H. Automated detection and classification of vascular abnormalities in diabetic retinopathy. In: *Conference Record of the Thirty-Eighth Asilomar Conference on Signals, Systems and Computers, 2004.*; vol. 2. IEEE; 2004, p. 1625–9.
- [29] Williams R, Airey M, Baxter H, Forrester Jm, Kennedy-Martin T, Girach A. Epidemiology of diabetic retinopathy and macular oedema: a systematic review. *Eye* 2004;18(10):963–83.
- [30] Giancardo L, Meriaudeau F, Karnowski TP, Li Y, Garg S, Tobin Jr KW, et al. Exudate-based diabetic macular edema detection in fundus images using publicly available datasets. *Medical image analysis* 2012;16(1):216–26.
- [31] Taylor SR, Lightman SL, Sugar EA, Jaffe GJ, Freeman WR, Altaweel MM, et al. The impact of macular edema on visual function in intermediate, posterior, and panuveitis. *Ocular immunology and inflammation* 2012;20(3):171–81.

- [32] Molina-Casado JM, Carmona EJ, Garcia-Feijoo J. Fast detection of the main anatomical structures in digital retinal images based on intra-and inter-structure relational knowledge. *Computer methods and programs in biomedicine* 2017;149:55–68.
- [33] Moccia S, De Momi E, El Hadji S, Mattos LS. Blood vessel segmentation algorithms review of methods, datasets and evaluation metrics. *Computer Methods and Programs in Biomedicine* 2018;158:71–91.
- [34] Wilkinson C, Ferris III FL, Klein RE, Lee PP, Agardh CD, Davis M, et al. Proposed international clinical diabetic retinopathy and diabetic macular edema disease severity scales. *Ophthalmology* 2003;110(9):1677–82.
- [35] Group ETDRSR, et al. Classification of diabetic retinopathy from fluorescein angiograms: Etdrs report number 11. *Ophthalmology* 1991;98(5):807–22.
- [36] Philip S, Fleming AD, Goatman KA, Fonseca S, Mcnamee P, Scotland GS, et al. The efficacy of automated disease/no disease grading for diabetic retinopathy in a systematic screening programme. *British Journal of Ophthalmology* 2007;91(11):1512–7.
- [37] Salamat N, Missen MMS, Rashid A. Diabetic retinopathy techniques in retinal images: a review. *Artificial intelligence in medicine* 2019;97:168–88.
- [38] Venkatesan R, Chandakkar P, Li B, Li HK. Classification of diabetic retinopathy images using multi-class multiple-instance learning based on color correlogram features. In: 2012 Annual International Conference of the IEEE Engineering in Medicine and Biology Society. IEEE; 2012, p. 1462–5.
- [39] Patton N, Aslam TM, MacGillivray T, Deary IJ, Dhillon B, Eikelboom RH, et al. Retinal image analysis: concepts, applications and potential. *Progress in retinal and eye research* 2006;25(1):99–127.
- [40] Kanski JJ. *Clinical ophthalmology: a synopsis*. Elsevier Health Sciences; 2009.
- [41] Zachariah S, Wykes W, Yorston D. Grading diabetic retinopathy (dr) using the scottish grading protocol. *Community eye health* 2015;28(92):72.
- [42] Scanlon PH. The english national screening programme for diabetic retinopathy 2003– 2016. *Acta diabetologica* 2017;54(6):515–25.

- [43] Ciulla TA, Amador AG, Zinman B. Diabetic retinopathy and diabetic macular edema: pathophysiology, screening, and novel therapies. *Diabetes care* 2003;26(9):2653–64.
- [44] Abramoff MD, Garvin MK, Sonka M. Retinal imaging and image analysis. *IEEE reviews in biomedical engineering* 2010;3:169–208.
- [45] Kauppi T, Kalesnykiene V, Kamarainen JK, Lensu L, Sorri I, Raninen A, et al. The diaretdb1 diabetic retinopathy database and evaluation protocol. In: *BMVC*; vol. 1. 2007, p. 1–10.
- [46] Budai A, Bock R, Maier A, Hornegger J, Michelson G. Robust vessel segmentation in fundus images. *International journal of biomedical imaging* 2013;2013.
- [47] Hoover A, Kouznetsova V, Goldbaum M. Locating blood vessels in retinal images by piecewise threshold probing of a matched filter response. *IEEE Transactions on Medical imaging* 2000;19(3):203–10.
- [48] Niemeijer M, Van Ginneken B, Cree MJ, Mizutani A, Quellec G, Sañchez CI, et al. Retinopathy online challenge: automatic detection of microaneurysms in digital color fundus photographs. *IEEE transactions on medical imaging* 2009;29(1):185–95.
- [49] Niemeijer M, Staal J, van Ginneken B, Loog M, Abramoff MD. Comparative study of retinal vessel segmentation methods on a new publicly available database. In: *SPIE Medical Imaging*; vol. 5370. SPIE; 2004, p. 648–56.
- [50] Decencière E, Zhang X, Cazuguel G, Lay B, Cochener B, Trone C, et al. Feedback on a publicly distributed image database: the messidor database. *Image Analysis & Stereology* 2014;33(3):231–4.
- [51] Decencière E, Cazuguel G, Zhang X, Thibault G, Klein JC, Meyer F, et al. Teleophta: Machine learning and image processing methods for teleophthalmology. *Irbm* 2013;34(2):196–203.
- [52] Fraz MM, Remagnino P, Hoppe A, Uyyanonvara B, Rudnicka AR, Owen CG, et al. Blood vessel segmentation methodologies in retinal images—a survey. *Computer Methods and Programs in Biomedicine* 2012;108(1):407–33.
- [53] Pourreza-Shahri R, Tavakoli M, Kehtarnavaz N. Computationally efficient optic nerve head detection in retinal fundus images. *Biomedical Signal Processing and Control* 2014;11:63–73.

- [54] Kaggle retinal database. <https://www.kaggle.com/c/diabetic-retinopathy-detection/data>. Accessed; ????. Accessed: 2018-01-08.
- [55] E-ophtha retinal database. <http://www.adcis.net/en/Download-Third-Party/E-Ophtha.html>. Accessed; ????. Accessed: 2018-01-08.
- [56] Fraz MM, Remagnino P, Hoppe A, Uyyanonvara B, Rudnicka AR, Owen CG, et al. An ensemble classification-based approach applied to retinal blood vessel segmentation. *IEEE Transactions on Biomedical Engineering* 2012;59(9):2538–48.
- [57] Aria retinal database. [http://www.eyecharity.com/aria\\_online.html](http://www.eyecharity.com/aria_online.html). Accessed; ????. Accessed: 2018-02-28.
- [58] Seed-db retinal database. <https://www.seri.com.sg/key-programmes/singapore-epidemiology-of-eye-diseases-seed/>. Accessed; ????. Accessed: 2018-08-08.
- [59] EyePACS retinal database. <http://www.eyepacs.com/eyepacssystem/>. Accessed; ????. Accessed: 2018-03-01.
- [60] Zhang Z, Yin FS, Liu J, Wong WK, Tan NM, Lee BH, et al. Origa-light: An online retinal fundus image database for glaucoma analysis and research. In: 2010 Annual International Conference of the IEEE Engineering in Medicine and Biology. IEEE; 2010, p. 3065–8.
- [61] Esmaeili M, Rabbani H, Dehnavi AM. Automatic optic disk boundary extraction by the use of curvelet transform and deformable variational level set model. *Pattern Recognition* 2012;45(7):2832–42.
- [62] Qureshi RJ, Kovacs L, Harangi B, Nagy B, Peto T, Hajdu A. Combining algorithms for automatic detection of optic disc and macula in fundus images. *Computer Vision and Image Understanding* 2012;116(1):138–45.
- [63] Welfer D, Scharcanski J, Marinho DR. A morphologic two-stage approach for automated optic disk detection in color eye fundus images. *Pattern Recognition Letters* 2013;34(5):476–85.
- [64] Harangi B, Hajdu A. Detection of the optic disc in fundus images by combining probability models. *Computers in biology and medicine* 2015;65:10–24.

- [65] Akyol K, Sen B, Bayir S. Automatic detection of optic disc in retinal image by using keypoint detection, texture analysis, and visual dictionary techniques. *Computational and mathematical methods in medicine* 2016;2016.
- [66] Dai B, Wu X, Bu W. Optic disc segmentation based on variational model with multiple energies. *Pattern Recognition* 2017;64:226–35.
- [67] Alshayeji M, Al-Roomi SA, et al. Optic disc detection in retinal fundus images using gravitational law-based edge detection. *Medical & biological engineering & computing* 2017;55(6):935–48.
- [68] Basit A, Fraz MM. Optic disc detection and boundary extraction in retinal images. *Applied optics* 2015;54(11):3440–7.
- [69] Hsu W, Pallawala P, Lee ML, Eong KGA. The role of domain knowledge in the detection of retinal hard exudates. In: *Proceedings of the 2001 IEEE Computer Society Conference on Computer Vision and Pattern Recognition. CVPR 2001; vol. 2. IEEE; 2001, p. II–.*
- [70] Niemeijer M, Abramoff MD, Van Ginneken B. Information fusion for diabetic retinopathy cad in digital color fundus photographs. *IEEE transactions on medical imaging* 2009;28(5):775–85.
- [71] Quellec G, Russell SR, Abramoff MD. Optimal filter framework for automated, instantaneous detection of lesions in retinal images. *IEEE transactions on medical imaging* 2010;30(2):523–33.
- [72] Amel F, Mohammed M, Abdelhafid B. Improvement of the hard exudates detection method used for computer-aided diagnosis of diabetic retinopathy. *International Journal of Image, Graphics & Signal Processing* 2012;4(4).
- [73] Sánchez CI, Niemeijer M, Dumitrescu AV, Suttorp-Schulten MS, Abramoff MD, van Ginneken B. Evaluation of a computer-aided diagnosis system for diabetic retinopathy screening on public data. *Investigative ophthalmology & visual science* 2011;52(7):4866–71.
- [74] Mansour RF. Evolutionary computing enriched computer-aided diagnosis system for diabetic retinopathy: a survey. *IEEE reviews in biomedical engineering* 2017;10:334–49.
- [75] Kumar D, Taylor GW, Wong A. Discovery radiomics with clear-dr: Interpretable computer aided diagnosis of diabetic retinopathy. *IEEE Access* 2019;7:25891–6.

- [76] Ganesan K, Martis RJ, Acharya UR, Chua CK, Min LC, Ng E, et al. Computeraided diabetic retinopathy detection using trace transforms on digital fundus images. *Medical & biological engineering & computing* 2014;52(8):663–72.
- [77] Sim DA, Keane PA, Tufail A, Egan CA, Aiello LP, Silva PS. Automated retinal image analysis for diabetic retinopathy in telemedicine. *Current diabetes reports* 2015;15(3):14.
- [78] Mandrekar JN. Receiver operating characteristic curve in diagnostic test assessment. *Journal of Thoracic Oncology* 2010;5(9):1315–6.
- [79] Marín D, Aquino A, Gegúndez-Arias ME, Bravo JM. A new supervised method for blood vessel segmentation in retinal images by using gray-level and moment invariantsbased features. *IEEE transactions on medical imaging* 2010;30(1):146–58.
- [80] Yan Z, Yang X, Cheng KT. A skeletal similarity metric for quality evaluation of retinal vessel segmentation. *IEEE transactions on medical imaging* 2017;37(4):1045–57.
- [81] Bharkad S. Automatic segmentation of optic disk in retinal images. *Biomedical Signal Processing and Control* 2017;31:483–98.
- [82] Leontidis G, Al-Diri B, Hunter A. A new unified framework for the early detection of the progression to diabetic retinopathy from fundus images. *Computers in biology and medicine* 2017;90:98–115.
- [83] Zou B, Chen C, Zhu C, Duan X, Chen Z. Classified optic disc localization algorithm based on verification model. *Computers & Graphics* 2018;70:281–7.
- [84] Xiong L, Li H. An approach to locate optic disc in retinal images with pathological changes. *Computerized Medical Imaging and Graphics* 2016;47:40–50.
- [85] Sarathi MP, Dutta MK, Singh A, Travieso CM. Blood vessel inpainting based technique for efficient localization and segmentation of optic disc in digital fundus images. *Biomedical Signal Processing and Control* 2016;25:108–17.
- [86] Lu S. Accurate and efficient optic disc detection and segmentation by a circular transformation. *IEEE Transactions on medical imaging* 2011;30(12):2126–33.
- [87] Lowell J, Hunter A, Steel D, Basu A, Ryder R, Fletcher E, et al. Optic nerve head segmentation. *IEEE Transactions on medical Imaging* 2004;23(2):256–64.

- [88] Hoover A, Goldbaum M. Locating the optic nerve in a retinal image using the fuzzy convergence of the blood vessels. *IEEE transactions on medical imaging* 2003;22(8):951–8.
- [89] Dash J, Bhoi N. A thresholding based technique to extract retinal blood vessels from fundus images. *Future Computing and Informatics Journal* 2017;2(2):103–9.
- [90] Zhu C, Zou B, Zhao R, Cui J, Duan X, Chen Z, et al. Retinal vessel segmentation in colour fundus images using extreme learning machine. *Computerized Medical Imaging and Graphics* 2017;55:68–77.
- [91] Neto LC, Ramalho GL, Neto JFR, Veras RM, Medeiros FN. An unsupervised coarse-to-fine algorithm for blood vessel segmentation in fundus images. *Expert Systems with Applications* 2017;78:182–92.
- [92] Xu L, Luo S. A novel method for blood vessel detection from retinal images. *Biomedical engineering online* 2010;9(1):14.
- [93] Nguyen UT, Bhuiyan A, Park LA, Ramamohanarao K. An effective retinal blood vessel segmentation method using multi-scale line detection. *Pattern Recognition* 2013;46(3):703–15.
- [94] Zhang L, Fisher M, Wang W. Retinal vessel segmentation using multi-scale textons derived from keypoints. *Computerized Medical Imaging and Graphics* 2015;45:47–56.
- [95] Fraz MM, Barman S, Remagnino P, Hoppe A, Basit A, Uyyanonvara B, et al. An approach to localize the retinal blood vessels using bit planes and centerline detection. *Computer Methods and Programs in Biomedicine* 2012;108(2):600–16.
- [96] Marín D, Aquino A, Gegúndez-Arias ME, Bravo JM. A new supervised method for blood vessel segmentation in retinal images by using gray-level and moment invariants based features. *IEEE Transactions on Medical Imaging* 2011;30(1):146–58.
- [97] Akram MU, Khan SA. Multilayered thresholding-based blood vessel segmentation for screening of diabetic retinopathy. *Engineering with Computers* 2013;29(2):165–73.
- [98] Vermeer KA, Vos FM, Lemij HG, Vossepoel AM. A model based method for retinal blood vessel detection. *Computers in Biology and Medicine* 2004;34(3):209–19.

- [99] Chakraborti T, Jha DK, Chowdhury AS, Jiang X. A self-adaptive matched filter for retinal blood vessel detection. *Machine Vision and Applications* 2015;26(1):55–68.
- [100] Wu D, Zhang M, Liu JC, Bauman W. On the adaptive detection of blood vessels in retinal images. *IEEE Transactions on Biomedical Engineering* 2006;53(2):341–3.
- [101] Tavakoli M, Mehdizadeh A, Pourreza R, Pourreza HR, Banaee T, Toosi MB. Radon transform technique for linear structures detection: application to vessel detection in fluorescein angiography fundus images. In: 2011 IEEE Nuclear Science Symposium Conference Record. IEEE; 2011, p. 3051–6.
- [102] Roychowdhury S, Koozekanani DD, Parhi KK. Blood vessel segmentation of fundus images by major vessel extraction and subimage classification. *IEEE Journal of Biomedical and Health Informatics* 2015;19(3):1118–28.
- [103] Toliyas YA, Panas SM. A fuzzy vessel tracking algorithm for retinal images based on fuzzy clustering. *IEEE Transactions on Medical Imaging* 1998;17(2):263–73.
- [104] Azzopardi G, Strisciuglio N, Vento M, Petkov N. Trainable cosfire filters for vessel delineation with application to retinal images. *Medical Image Analysis* 2015;19(1):46– 57.
- [105] Zana F, Klein JC. A multimodal registration algorithm of eye fundus images using vessels detection and hough transform. *IEEE Transactions on Medical Imaging* 1999;18(5):419–28.
- [106] Zana F, Klein JC. Segmentation of vessel-like patterns using mathematical morphology and curvature evaluation. *IEEE Transactions on Image Processing* 2001;10(7):1010–9.
- [107] Soares JV, Leandro JJ, Cesar RM, Jelinek HF, Cree MJ. Retinal vessel segmentation using the 2-d gabor wavelet and supervised classification. *IEEE Transactions on Medical Imaging* 2006;25(9):1214–22.
- [108] Quellec G, Lamard M, Josselin PM, Cazuguel G, Cochener B, Roux C. Optimal wavelet transform for the detection of microaneurysms in retina photographs. *IEEE Transactions on Medical Imaging* 2008;27(9):1230–41.
- [109] Wang S, Tang HL, Hu Y, Sanei S, Saleh GM, Peto T, et al. Localizing microaneurysms in fundus images through singular spectrum analysis. *IEEE Transactions on Biomedical Engineering* 2016;64(5):990–1002.

- [110] Srivastava R, Duan L, Wong DW, Liu J, Wong TY. Detecting retinal microaneurysms and hemorrhages with robustness to the presence of blood vessels. *Computer methods and programs in biomedicine* 2017;138:83–91.
- [111] Dai L, Fang R, Li H, Hou X, Sheng B, Wu Q, et al. Clinical report guided retinal microaneurysm detection with multi-sieving deep learning. *IEEE Transactions on Medical Imaging* 2018;37(5):1149–61.
- [112] van Grinsven MJ, van Ginneken B, Hoyng CB, Theelen T, Sa´nchez CI. Fast convolutional neural network training using selective data sampling: Application to hemorrhage detection in color fundus images. *IEEE Transactions on Medical Imaging* 2016;35(5):1273–84.
- [113] Pereira C, Veiga D, Mahdjoub J, Guessoum Z, Goncalves L, Ferreira M, et al. Using a multi-agent system approach for microaneurysm detection in fundus images. *Artificial intelligence in medicine* 2014;60(3):179–88.
- [114] Liu Q, Zou B, Chen J, Ke W, Yue K, Chen Z, et al. A location-to-segmentation strategy for automatic exudate segmentation in colour retinal fundus images. *Computerized medical imaging and graphics* 2017;55:78–86.
- [115] Orlando JI, Prokofyeva E, del Fresno M, Blaschko MB. An ensemble deep learning based approach for red lesion detection in fundus images. *Computer methods and programs in biomedicine* 2018;153:115–27.
- [116] Zhang X, Thibault G, Decenciere E, Marcotegui B, Lay B, Danno R, et al. Exudate detection in color retinal images for mass screening of diabetic retinopathy. *Medical image analysis* 2014;18(7):1026–43.
- [117] Youssef D, Solouma NH. Accurate detection of blood vessels improves the detection of exudates in color fundus images. *Computer methods and programs in biomedicine* 2012;108(3):1052–61.
- [118] Fraz MM, Jahangir W, Zahid S, Hamayun MM, Barman SA. Multiscale segmentation of exudates in retinal images using contextual cues and ensemble classification. *Biomedical Signal Processing and Control* 2017;35:50–62.
- [119] Amin J, Sharif M, Yasmin M, Ali H, Fernandes SL. A method for the detection and classification of diabetic retinopathy using structural predictors of bright lesions. *Journal of Computational Science* 2017;19:153–64.

- [120] Sopharak A, Uyyanonvara B, Barman S. Automatic exudate detection for diabetic retinopathy screening. *Science Asia* 2009;35(1):80–8.
- [121] Sánchez CI, García M, Mayo A, López MI, Hornero R. Retinal image analysis based on mixture models to detect hard exudates. *Medical Image Analysis* 2009;13(4):650–8.
- [122] Koh JE, Acharya UR, Hagiwara Y, Raghavendra U, Tan JH, Sree SV, et al. Diagnosis of retinal health in digital fundus images using continuous wavelet transform (cwt) and entropies. *Computers in biology and medicine* 2017;84:89–97.
- [123] Gardner G, Keating D, Williamson T, Elliott A. Automatic detection of diabetic retinopathy using an artificial neural network: a screening tool. *British Journal of Ophthalmology* 1996;80(11):940–4.
- [124] Rubini SS, Kunthavai A. Diabetic retinopathy detection based on eigenvalues of the hessian matrix. *Procedia Computer Science* 2015;47:311–8.
- [125] Gulshan V, Peng L, Coram M, Stumpe MC, Wu D, Narayanaswamy A, et al. Development and validation of a deep learning algorithm for detection of diabetic retinopathy in retinal fundus photographs. *Jama* 2016;316(22):2402–10.
- [126] Köse C, Şevik U, Kibas C, Erdoğ H. Simple methods for segmentation and measurement of diabetic retinopathy lesions in retinal fundus images. *Computer methods and programs in biomedicine* 2012;107(2):274–93.
- [127] Yang Y, Li T, Li W, Wu H, Fan W, Zhang W. Lesion detection and grading of diabetic retinopathy via two-stages deep convolutional neural networks. In: *International Conference on Medical Image Computing and Computer-Assisted Intervention*. Springer; 2017, p. 533–40.
- [128] Sisodia DS, Nair S, Khobragade P. Diabetic retinal fundus images: Preprocessing and feature extraction for early detection of diabetic retinopathy. *Biomedical and Pharmacology Journal* 2017;10(2):615–26.
- [129] Kumar PS, Deepak R, Sathar A, Sahasranamam V, Kumar RR. Automated detection system for diabetic retinopathy using two field fundus photography. *Procedia computer science* 2016;93:486–94.

- [130] Gupta G, Kulasekaran S, Ram K, Joshi N, Sivaprakasam M, Gandhi R. Local characterization of neovascularization and identification of proliferative diabetic retinopathy in retinal fundus images. *Computerized Medical Imaging and Graphics* 2017;55:124–32.
- [131] Sinthanayothin C, Kongbunkiat V, Phoojaruenchanachai S, Singalavanija A. Automated screening system for diabetic retinopathy. In: 3rd International Symposium on Image and Signal Processing and Analysis, 2003. ISPA 2003. Proceedings of the; vol. 2. IEEE; 2003, p. 915–20.
- [132] Usher D, Dumskyj M, Himaga M, Williamson TH, Nussey S, Boyce J. Automated detection of diabetic retinopathy in digital retinal images: a tool for diabetic retinopathy screening. *Diabetic Medicine* 2004;21(1):84–90.
- [133] Fleming A, Goatman K, Williams G, Philip S, Sharp P, Olson J. Automated detection of blot haemorrhages as a sign of referable diabetic retinopathy. In: *Proc. Medical Image Understanding and Analysis*. 2008,.
- [134] Perumalsamy N, Prasad NM, Sathya S, Ramasamy K. Software for reading and grading diabetic retinopathy: Aravind diabetic retinopathy screening 3.0. *Diabetes care* 2007;30(9):2302–6.
- [135] Winder RJ, Morrow PJ, McRitchie IN, Bailie J, Hart PM. Algorithms for digital image processing in diabetic retinopathy. *Computerized medical imaging and graphics* 2009;33(8):608–22.
- [136] Mookiah MRK, Acharya UR, Martis RJ, Chua CK, Lim CM, Ng E, et al. Evolutionary algorithm based classifier parameter tuning for automatic diabetic retinopathy grading: A hybrid feature extraction approach. *Knowledge-based systems* 2013;39:9–22.
- [137] Abramoff MD, Suttrop-Schulten MS. Web-based screening for diabetic retinopathy in a primary care population: the eyecheck project. *Telemedicine Journal & e-Health* 2005;11(6):668–74.
- [138] Abramoff MD, Niemeijer M, Suttrop-Schulten MS, Viergever MA, Russell SR, Van Ginneken B. Evaluation of a system for automatic detection of diabetic retinopathy from color fundus photographs in a large population of patients with diabetes. *Diabetes care* 2008;31(2):193–8.
- [139] Teng T, Lefley M, Claremont D. Progress towards automated diabetic ocular screening:

- a review of image analysis and intelligent systems for diabetic retinopathy. *Medical and Biological Engineering and Computing* 2002;40(1):2–13.
- [140] Wang H, Hsu W, Goh KG, Lee ML. An effective approach to detect lesions in color retinal images. In: *Proceedings IEEE Conference on Computer Vision and Pattern Recognition. CVPR 2000 (Cat. No. PR00662); vol. 2. IEEE; 2000, p. 181–6.*
- [141] Singalavanija A, Supokavej J, Bamroongsuk P, Sinthanayothin C, Phoojaruenchanachai S, Kongbunkiat V. Feasibility study on computer-aided screening for diabetic retinopathy. *Japanese journal of ophthalmology* 2006;50(4):361–6.
- [142] Gang L, Chutatape O, Krishnan SM. Detection and measurement of retinal vessels in fundus images using amplitude modified second-order gaussian filter. *IEEE transactions on Biomedical Engineering* 2002;49(2):168–72.
- [143] Kahai P, Namuduri KR, Thompson H. A decision support framework for automated screening of diabetic retinopathy. *International journal of biomedical imaging* 2006;2006.
- [144] Yun WL, Acharya UR, Venkatesh YV, Chee C, Min LC, Ng EYK. Identification of different stages of diabetic retinopathy using retinal optical images. *Information sciences* 2008;178(1):106–21.
- [145] Acharya UR, Lim CM, Ng EYK, Chee C, Tamura T. Computer-based detection of diabetes retinopathy stages using digital fundus images. *Proceedings of the institution of mechanical engineers, part H: journal of engineering in medicine* 2009;223(5):545–53.
- [146] Larsen N, Godt J, Grunkin M, Lund-Andersen H, Larsen M. Automated detection of diabetic retinopathy in a fundus photographic screening population. *Investigative ophthalmology & visual science* 2003;44(2):767–71.
- [147] Joshi GD, Sivaswamy J, Krishnadas S. Optic disk and cup segmentation from monocular color retinal images for glaucoma assessment. *IEEE transactions on medical imaging* 2011;30(6):1192–205.
- [148] Tavakoli M, Kelley P, Nazar M, Kalantari F. Automated fovea detection based on unsupervised retinal vessel segmentation method. In: *2017 IEEE Nuclear Science Symposium and Medical Imaging Conference (NSS/MIC). IEEE; 2017, p. 1–7.*

- [149] Sinthanayothin C. Image analysis for automatic diagnosis of diabetic retinopathy. Ph D Thesis, Department of Physics, King's College London 1999;.
- [150] Gagnon L, Lalonde M, Beaulieu M, Boucher MC. Procedure to detect anatomical structures in optical fundus images. In: Medical imaging 2001: Image processing; vol. 4322. International Society for Optics and Photonics; 2001, p. 1218–25.
- [151] Hubbard LD, Brothers RJ, King WN, Clegg LX, Klein R, Cooper LS, et al. Methods for evaluation of retinal microvascular abnormalities associated with hypertension/sclerosis in the atherosclerosis risk in communities study. *Ophthalmology* 1999;106(12):2269–80.
- [152] Kamble R, Kokare M, Deshmukh G, Hussin FA, M'eriaudeau F. Localization of optic disc and fovea in retinal images using intensity based line scanning analysis. *Computers in biology and medicine* 2017;87:382–96.
- [153] Elbalaoui A, Fakir M, Boutaounte M, Merbouha A. Automatic localization of the optic disc center in retinal images based on angle detection in curvature scale space. In: *Medical Imaging: Concepts, Methodologies, Tools, and Applications*. IGI Global; 2017, p. 679–92.
- [154] Unver HM, K'okver Y, Duman E, Erdem OA. Statistical edge detection and circular' hough transform for optic disk localization. *Applied Sciences* 2019;9(2):350.
- [155] Meng X, Xi X, Yang L, Zhang G, Yin Y, Chen X. Fast and effective optic disk localization based on convolutional neural network. *Neurocomputing* 2018;312:285–95.
- [156] Muangnak N, Aimmanee P, Makhanov S. Automatic optic disk detection in retinal images using hybrid vessel phase portrait analysis. *Medical & biological engineering & computing* 2018;56(4):583–98.
- [157] Lalonde M, Gagnon L, Boucher MC. Non-recursive paired tracking for vessel extraction from retinal images. In: *Vision interface*. 2000, p. 61–8.
- [158] Zahoor MN, Fraz MM. Fast optic disc segmentation in retina using polar transform. *IEEE Access* 2017;5:12293–300.
- [159] Manju K, Sabeenian R, Surendar A. A review on optic disc and cup segmentation. *Biomedical and Pharmacology Journal* 2017;10(1):373–9.

- [160] Rodrigues LC, Marengoni M. Segmentation of optic disc and blood vessels in retinal images using wavelets, mathematical morphology and hessian-based multi-scale filtering. *Biomedical Signal Processing and Control* 2017;36:39–49.
- [161] Rehman ZU, Naqvi SS, Khan TM, Arsalan M, Khan MA, Khalil M. Multi-parametric optic disc segmentation using superpixel based feature classification. *Expert Systems with Applications* 2019;120:461–73.
- [162] Goldbaum M, Moezzi S, Taylor A, Chatterjee S, Boyd J, Hunter E, et al. Automated diagnosis and image understanding with object extraction, object classification, and inferencing in retinal images. In: *Proceedings of 3rd IEEE international conference on image processing*; vol. 3. IEEE; 1996, p. 695–8.
- [163] Sinthanayothin C, Boyce JF, Cook HL, Williamson TH. Automated localisation of the optic disc, fovea, and retinal blood vessels from digital colour fundus images. *British journal of ophthalmology* 1999;83(8):902–10.
- [164] Walter T, Klein JC. Segmentation of color fundus images of the human retina: Detection of the optic disc and the vascular tree using morphological techniques. In: *International Symposium on Medical Data Analysis*. Springer; 2001, p. 282–7.
- [165] Tavakoli M, Nazar M, Golestaneh A, Kalantari F. Automated optic nerve head detection based on different retinal vasculature segmentation methods and mathematical morphology. In: *2017 IEEE Nuclear Science Symposium and Medical Imaging Conference (NSS/MIC)*. IEEE; 2017, p. 1–7.
- [166] Chr´astek R, Wolf M, Donath K, Niemann H, Paulus D, Hothorn T, et al. Automated segmentation of the optic nerve head for diagnosis of glaucoma. *Medical image analysis* 2005;9(4):297–314.
- [167] Abdel-Ghafar R, Morris T. Progress towards automated detection and characterization of the optic disc in glaucoma and diabetic retinopathy. *Medical informatics and the Internet in medicine* 2007;32(1):19–25.
- [168] Tavakoli M, Toosi MB, Pourreza R, Banaee T, Pourreza HR. Automated optic nerve head detection in fluorescein angiography fundus images. In: *2011 IEEE Nuclear Science Symposium Conference Record*. IEEE; 2011, p. 3057–60.

- [169] S´anchez CI, Hornero R, Lopez MI, Poza J. Retinal image analysis to detect and quantify lesions associated with diabetic retinopathy. In: The 26th Annual International Conference of the IEEE Engineering in Medicine and Biology Society; vol. 1. IEEE; 2004, p. 1624–7.
- [170] Li H, Chutatape O. Automated feature extraction in color retinal images by a model based approach. IEEE Transactions on biomedical engineering 2004;51(2):246–54.
- [171] Foracchia M, Grisan E, Ruggeri A. Detection of optic disc in retinal images by means of a geometrical model of vessel structure. IEEE transactions on medical imaging 2004;23(10):1189–95.
- [172] Youssif AAHAR, Ghalwash AZ, Ghoneim AASAR. Optic disc detection from normalized digital fundus images by means of a vessels’ direction matched filter. IEEE transactions on medical imaging 2007;27(1):11–8.
- [173] Lu S, Lim JH. Automatic optic disc detection from retinal images by a line operator. IEEE Transactions on Biomedical Engineering 2010;58(1):88–94.
- [174] Li H, Chutatape O. Automatic location of optic disk in retinal images. In: Proceedings 2001 International Conference on Image Processing (Cat. No. 01CH37205); vol. 2. IEEE; 2001, p. 837–40.
- [175] Li H, Chutatape O. A model-based approach for automated feature extraction in fundus images. In: null. IEEE; 2003, p. 394.
- [176] Osareh A, Mirmehdi M, Thomas B, Markham R. Comparison of colour spaces for optic disc localisation in retinal images. In: Object recognition supported by user interaction for service robots; vol. 1. IEEE; 2002, p. 743–6.
- [177] Osareh A, Mirmehdi M, Thomas B, Markham R. Classification and localisation of diabetic-related eye disease. In: European Conference on Computer Vision. Springer; 2002, p. 502–16.
- [178] Xu J, Chutatape O, Sung E, Zheng C, Kuan PCT. Optic disk feature extraction via modified deformable model technique for glaucoma analysis. Pattern recognition 2007;40(7):2063–76.
- [179] Wong D, Liu J, Lim J, Jia X, Yin F, Li H, et al. Level-set based automatic cup-to-disc ratio determination using retinal fundus images in argali. In: 2008 30th Annual International

- Conference of the IEEE Engineering in Medicine and Biology Society. IEEE; 2008, p. 2266–9.
- [180] Lalonde M, Beaulieu M, Gagnon L. Fast and robust optic disc detection using pyramidal decomposition and hausdorff-based template matching. *IEEE transactions on medical imaging* 2001;20(11):1193–200.
- [181] Ter Haar F. Automatic localization of the optic disc in digital colour images of the human retina. Utrecht University 2005;.
- [182] Tobin KW, Chaum E, Govindasamy VP, Karnowski TP. Detection of anatomic structures in human retinal imagery. *IEEE transactions on medical imaging* 2007;26(12):1729–39.
- [183] Niemeijer M, Abramoff MD, Van Ginneken B. Fast detection of the optic disc and fovea in color fundus photographs. *Medical image analysis* 2009;13(6):859–70.
- [184] Fleming AD, Goatman KA, Philip S, Olson JA, Sharp PF. Automatic detection of retinal anatomy to assist diabetic retinopathy screening. *Physics in Medicine & Biology* 2006;52(2):331.
- [185] Niemeijer M, Abramoff MD, Van Ginneken B. Segmentation of the optic disc, macula and vascular arch in fundus photographs. *IEEE transactions on medical imaging* 2006;26(1):116–27.
- [186] Abramoff MD, Niemeijer M. The automatic detection of the optic disc location in retinal images using optic disc location regression. In: 2006 International Conference of the IEEE Engineering in Medicine and Biology Society. IEEE; 2006, p. 4432–5.
- [187] Abramoff MD, Alward WL, Greenlee EC, Shuba L, Kim CY, Fingert JH, et al. Automated segmentation of the optic disc from stereo color photographs using physiologically plausible features. *Investigative ophthalmology & visual science* 2007;48(4):1665–73.
- [188] Hsiao HK, Liu CC, Yu CY, Kuo SW, Yu SS. A novel optic disc detection scheme on retinal images. *Expert Systems with Applications* 2012;39(12):10600–6.
- [189] Yu H, Barriga ES, Agurto C, Echegaray S, Pattichis MS, Bauman W, et al. Fast localization and segmentation of optic disk in retinal images using directional matched filtering and level sets. *IEEE Transactions on information technology in biomedicine* 2012;16(4):644–57.

- [190] Mahfouz AE, Fahmy AS. Fast localization of the optic disc using projection of image features. *IEEE Transactions on Image Processing* 2010;19(12):3285–9.
- [191] Estrada R, Allingham MJ, Mettu PS, Cousins SW, Tomasi C, Farsiu S. Retinal arteryvein classification via topology estimation. *IEEE Transactions on Medical Imaging* 2015;34(12):2518–34.
- [192] Dashtbozorg B, Mendonca AM, Campilho A. An automatic graph-based approach for artery/vein classification in retinal images. *IEEE Transactions on Image Processing* 2014;23(3):1073–83.
- [193] Zhao YQ, Wang XH, Wang XF, Shih FY. Retinal vessels segmentation based on level set and region growing. *Pattern Recognition* 2014;47(7):2437–46.
- [194] Kovács G, Hajdu A. A self-calibrating approach for the segmentation of retinal vessels by template matching and contour reconstruction. *Medical Image Analysis* 2016;29:24–46.
- [195] Lázár I, Hajdu A. Segmentation of retinal vessels by means of directional response vector similarity and region growing. *Computers in Biology and Medicine* 2015;66:209–21.
- [196] Orlando JJ, Prokofyeva E, Blaschko MB. A discriminatively trained fully connected conditional random field model for blood vessel segmentation in fundus images. *IEEE Transactions on Biomedical Engineering* 2017;64(1):16–27.
- [197] Hassan M, Amin M, Murtza I, Khan A, Chaudhry A. Robust hidden markov model based intelligent blood vessel detection of fundus images. *Computer methods and programs in biomedicine* 2017;151:193–201.
- [198] Aslani S, Sarnel H. A new supervised retinal vessel segmentation method based on robust hybrid features. *Biomedical Signal Processing and Control* 2016;30:1–12.
- [199] Lupascu CA, Tegolo D, Trucco E. Fabc: retinal vessel segmentation using adaboost. *IEEE Transactions on Information Technology in Biomedicine* 2010;14(5):1267–74.
- [200] Vega R, Sanchez-Ante G, Falcon-Morales LE, Sossa H, Guevara E. Retinal vessel extraction using lattice neural networks with dendritic processing. *Computers in biology and medicine* 2015;58:20–30.

- [201] Waheed A, Akram MU, Khalid S, Waheed Z, Khan MA, Shaukat A. Hybrid features and methods classification based robust segmentation of blood vessels. *Journal of medical systems* 2015;39(10):128.
- [202] Zilly J, Buhmann JM, Mahapatra D. Glaucoma detection using entropy sampling and ensemble learning for automatic optic cup and disc segmentation. *Computerized Medical Imaging and Graphics* 2017;55:28–41.
- [203] Annunziata R, Garzelli A, Ballerini L, Mecocci A, Trucco E. Leveraging multiscale hessian-based enhancement with a novel exudate inpainting technique for retinal vessel segmentation. *IEEE Journal of Biomedical and Health Informatics* 2016;20(4):1129–38.
- [204] Mendonca AM, Campilho A. Segmentation of retinal blood vessels by combining the detection of centerlines and morphological reconstruction. *IEEE Transactions on Medical Imaging* 2006;25(9):1200–13.
- [205] Martinez-Perez ME, Hughes AD, Thom SA, Bharath AA, Parker KH. Segmentation of blood vessels from red-free and fluorescein retinal images. *Medical Image Analysis* 2007;11(1):47–61.
- [206] Zhang J, Dashtbozorg B, Bekkers E, Pluim JP, Duits R, ter Haar Romeny BM. Robust retinal vessel segmentation via locally adaptive derivative frames in orientation scores. *IEEE Transactions on Medical Imaging* 2016;35(12):2631–44.
- [207] Lam BSY, Yan H. A novel vessel segmentation algorithm for pathological retina images based on the divergence of vector fields. *IEEE Transactions on Medical Imaging* 2008;27(2):237–46.
- [208] Ricci E, Perfetti R. Retinal blood vessel segmentation using line operators and support vector classification. *IEEE Transactions on Medical Imaging* 2007;26(10):1357–65.
- [209] Wang Y, Lee SC. A fast method for automated detection of blood vessels in retinal images. In: *Signals, Systems & Computers, 1997. Conference Record of the ThirtyFirst Asilomar Conference on*; vol. 2. IEEE; 1997, p. 1700–4.
- [210] Jiang X, Mojon D. Adaptive local thresholding by verification-based multithreshold probing with application to vessel detection in retinal images. *IEEE Transactions on Pattern Analysis and Machine Intelligence* 2003;25(1):131–7.

- [211] Heneghan C, Flynn J, O'Keefe M, Cahill M. Characterization of changes in blood vessel width and tortuosity in retinopathy of prematurity using image analysis. *Medical Image Analysis* 2002;6(4):407–29.
- [212] Roychowdhury S, Koozekanani DD, Parhi KK. Iterative vessel segmentation of fundus images. *IEEE Transactions on Biomedical Engineering* 2015;62(7):1738–49.
- [213] Staal J, Abramoff MD, Niemeijer M, Viergever MA, Van Ginneken B. Ridge-based vessel segmentation in color images of the retina. *IEEE Transactions on Medical Imaging* 2004;23(4):501–9.
- [214] Li Q, Feng B, Xie L, Liang P, Zhang H, Wang T. A cross-modality learning approach for vessel segmentation in retinal images. *IEEE Transactions on Medical Imaging* 2016;35(1):109–18.
- [215] Annunziata R, Trucco E. Accelerating convolutional sparse coding for curvilinear structures segmentation by refining scirf-ts filter banks. *IEEE Transactions on Medical Imaging* 2016;35(11):2381–92.
- [216] Wang S, Yin Y, Cao G, Wei B, Zheng Y, Yang G. Hierarchical retinal blood vessel segmentation based on feature and ensemble learning. *Neurocomputing* 2015;149:708–17.
- [217] Tan JH, Acharya UR, Bhandary SV, Chua KC, Sivaprasad S. Segmentation of optic disc, fovea and retinal vasculature using a single convolutional neural network. *Journal of Computational Science* 2017;20:70–9.
- [218] Liskowski P, Krawiec K. Segmenting retinal blood vessels with deep neural networks. *IEEE Transactions on Medical Imaging* 2016;35(11):2369–80.
- [219] Yue K, Zou B, Chen Z, Liu Q. Retinal vessel segmentation using dense u-net with multiscale inputs. *Journal of Medical Imaging* 2019;6(3):034004.
- [220] Lin Y, Zhang H, Hu G. Automatic retinal vessel segmentation via deeply supervised and smoothly regularized network. *IEEE Access* 2018;.
- [221] Ren X, Zheng Y, Zhao Y, Luo C, Wang H, Lian J, et al. Drusen segmentation from retinal images via supervised feature learning. *IEEE Access* 2018;6:2952–61.
- [222] Oliveira A, Pereira S, Silva CA. Retinal vessel segmentation based on fully convolutional neural networks. *Expert Systems with Applications* 2018;112:229–42.

- [223] Singh N, Kaur L, Singh K. Segmentation of retinal blood vessels based on feature-oriented dictionary learning and sparse coding using ensemble classification approach. *Journal of Medical Imaging* 2019;6(4):044006.
- [224] Narasimha-Iyer H, Can A, Roysam B, Tanenbaum HL, Majerovics A. Integrated analysis of vascular and nonvascular changes from color retinal fundus image sequences. *IEEE Transactions on Biomedical Engineering* 2007;54(8):1436–45.
- [225] Goatman K, Charnley A, Webster L, Nussey S. Assessment of automated disease detection in diabetic retinopathy screening using two-field photography. *PLOS one* 2011;6(12).
- [226] Köse C, Şevik U, Gençaliog˘lu O. Automatic segmentation of age-related macular degeneration in retinal fundus images. *Computers in Biology and Medicine* 2008;38(5):611–9.
- [227] Zhou W, Wu C, Chen D, Yi Y, Du W. Automatic microaneurysm detection using the sparse principal component analysis-based unsupervised classification method. *IEEE access* 2017;5:2563–72.
- [228] Al-Bander B, Al-Nuaimy W, Williams BM, Zheng Y. Multiscale sequential convolutional neural networks for simultaneous detection of fovea and optic disc. *Biomedical Signal Processing and Control* 2018;40:91–101.
- [229] GeethaRamani R, Balasubramanian L. Macula segmentation and fovea localization employing image processing and heuristic based clustering for automated retinal screening. *Computer methods and programs in biomedicine* 2018;160:153–63.
- [230] Fadzil MA, Izhar LI, Nugroho HA. Determination of foveal avascular zone in diabetic retinopathy digital fundus images. *Computers in biology and medicine* 2010;40(7):657–64.
- [231] Acharya R, Ng YE, Suri JS. *Image modeling of the human eye*. Artech House; 2008.
- [232] Sekhar S, Al-Nuaimy W, Nandi AK. Automated localisation of retinal optic disk using hough transform. In: *2008 5th IEEE International Symposium on Biomedical Imaging: From Nano to Macro*. IEEE; 2008, p. 1577–80.
- [233] Welfer D, Scharcanski J, Marinho DR. Fovea center detection based on the retina anatomy and mathematical morphology. *Computer methods and programs in biomedicine* 2011;104(3):397–409.

- [234] Niemeijer M, Van Ginneken B, Staal J, Suttorp-Schulten MS, Abramoff MD. Automatic detection of red lesions in digital color fundus photographs. *IEEE Transactions on Medical Imaging* 2005;24(5):584–92.
- [235] Saleh MD, Eswaran C. An automated decision-support system for non-proliferative diabetic retinopathy disease based on mas and has detection. *Computer methods and programs in biomedicine* 2012;108(1):186–96.
- [236] Lazar I, Hajdu A. Retinal microaneurysm detection through local rotating cross-section profile analysis. *IEEE Transactions on Medical Imaging* 2013;32(2):400–7.
- [237] Dashtbozorg B, Zhang J, Huang F, ter Haar Romeny BM. Retinal microaneurysms detection using local convergence index features. *IEEE Transactions on Image Processing* 2018;27(7):3300–15.
- [238] Habib M, Welikala R, Hoppe A, Owen C, Rudnicka A, Barman S. Detection of microaneurysms in retinal images using an ensemble classifier. *Informatics in Medicine Unlocked* 2017;9:44–57.
- [239] Gegundez-Arias ME, Marin D, Ponte B, Alvarez F, Garrido J, Ortega C, et al. A tool for automated diabetic retinopathy pre-screening based on retinal image computer analysis. *Computers in biology and medicine* 2017;88:100–9.
- [240] Ram K, Joshi GD, Sivaswamy J. A successive clutter-rejection-based approach for early detection of diabetic retinopathy. *IEEE Transactions on Biomedical Engineering* 2010;58(3):664–73.
- [241] Mizutani A, Muramatsu C, Hatanaka Y, Suemori S, Hara T, Fujita H. Automated microaneurysm detection method based on double ring filter in retinal fundus images. In: *Medical Imaging 2009: Computer-Aided Diagnosis*; vol. 7260. International Society for Optics and Photonics; 2009, p. 72601N.
- [242] Ravishankar S, Jain A, Mittal A. Automated feature extraction for early detection of diabetic retinopathy in fundus images. In: *2009 IEEE Conference on Computer Vision and Pattern Recognition*. IEEE; 2009, p. 210–7.
- [243] Shah SAA, Laude A, Faye I, Tang TB. Automated microaneurysm detection in diabetic retinopathy using curvelet transform. *Journal of biomedical optics* 2016;21(10):101404.

- [244] Cao W, Czarnek N, Shan J, Li L. Microaneurysm detection using principal component analysis and machine learning methods. *IEEE transactions on nanobioscience* 2018;17(3):191–8.
- [245] Manjaramkar A, Kokare M. Statistical geometrical features for microaneurysm detection. *Journal of digital imaging* 2018;31(2):224–34.
- [246] Mumtaz R, Hussain M, Sarwar S, Khan K, Mumtaz S, Mumtaz M. Automatic detection of retinal hemorrhages by exploiting image processing techniques for screening retinal diseases in diabetic patients. *International Journal of Diabetes in Developing Countries* 2018;38(1):80–7.
- [247] Biran A, Bidari PS, Raahemifar K. Automatic method for exudates and hemorrhages detection from fundus retinal images. *International Journal of Computer and Information Engineering* 2016;10(9):1599–602.
- [248] Lahmiri S, Shmuel A. Variational mode decomposition based approach for accurate classification of color fundus images with hemorrhages. *Optics & Laser Technology* 2017;96:243–8.
- [249] Hatanaka Y, Nakagawa T, Hayashi Y, Kakogawa M, Sawada A, Kawase K, et al. Improvement of automatic hemorrhage detection methods using brightness correction on fundus images. In: *Medical Imaging 2008: Computer-Aided Diagnosis*; vol. 6915. International Society for Optics and Photonics; 2008, p. 69153E.
- [250] Spencer T, Olson JA, McHardy KC, Sharp PF, Forrester JV. An image-processing strategy for the segmentation and quantification of microaneurysms in fluorescein angiograms of the ocular fundus. *Computers and biomedical research* 1996;29(4):284–302.
- [251] Frame AJ, Undrill PE, Cree MJ, Olson JA, McHardy KC, Sharp PF, et al. A comparison of computer based classification methods applied to the detection of microaneurysms in ophthalmic fluorescein angiograms. *Computers in biology and medicine* 1998;28(3):225–38.
- [252] Zhang B, Wu X, You J, Li Q, Karray F. Detection of microaneurysms using multi-scale correlation coefficients. *Pattern Recognition* 2010;43(6):2237–48.

- [253] Zhang X, Chutatape O. A svm approach for detection of hemorrhages in background diabetic retinopathy. In: Proceedings. 2005 IEEE International Joint Conference on Neural Networks, 2005.; vol. 4. IEEE; 2005, p. 2435–40.
- [254] Hipwell J, Strachan F, Olson J, McHardy K, Sharp P, Forrester J. Automated detection of microaneurysms in digital red-free photographs: a diabetic retinopathy screening tool. *Diabetic medicine* 2000;17(8):588–94.
- [255] Antal B, Hajdu A. An ensemble-based system for microaneurysm detection and diabetic retinopathy grading. *IEEE transactions on biomedical engineering* 2012;59(6):1720–6.
- [256] Kusakunniran W, Wu Q, Ritthipravat P, Zhang J. Hard exudates segmentation based on learned initial seeds and iterative graph cut. *Computer methods and programs in biomedicine* 2018;158:173–83.
- [257] Zubair M, Ali H, Javed MY. Automated segmentation of hard exudates using dynamic thresholding to detect diabetic retinopathy in retinal photographs. *JMPT* 2016;7(3):109–16.
- [258] Lara Rodríguez LD, Urcid Serrano G. Exudates and blood vessel segmentation in eye fundus images using the fourier and cosine discrete transforms. *Computación y Sistemas* 2016;20(4):697–708.
- [259] Osareh A, Mirmehdi M, Thomas B, Markham R. Automated identification of diabetic retinal exudates in digital colour images. *British Journal of Ophthalmology* 2003;87(10):1220–3.
- [260] Osareh A, Shadgar B, Markham R. A computational-intelligence-based approach for detection of exudates in diabetic retinopathy images. *IEEE Transactions on Information Technology in Biomedicine* 2009;13(4):535–45.
- [261] Bezdek JC. *Pattern recognition with fuzzy objective function algorithms*. Springer Science & Business Media; 2013.
- [262] Sopharak A, Nwe KT, Moe YA, Dailey MN, Uyyanonvara B, et al. Automatic exudate detection with a naive bayes classifier. In: *International Conference on Embedded Systems and Intelligent Technology*. 2008, p. 139–42.
- [263] Sopharak A, Uyyanonvara B, Barman S, Williamson TH. Automatic detection of diabetic retinopathy exudates from non-dilated retinal images using mathematical morphology methods. *Computerized medical imaging and graphics* 2008;32(8):720–7.

- [264] Walter T, Klein JC, Massin P, Erginay A. A contribution of image processing to the diagnosis of diabetic retinopathy-detection of exudates in color fundus images of the human retina. *IEEE transactions on medical imaging* 2002;21(10):1236–43.
- [265] Welfer D, Scharcanski J, Marinho DR. A coarse-to-fine strategy for automatically detecting exudates in color eye fundus images. *computerized medical imaging and graphics* 2010;34(3):228–35.
- [266] S´anchez CI, Hornero R, Lo´pez MI, Aboy M, Poza J, Aba´solo D. A novel automatic image processing algorithm for detection of hard exudates based on retinal image analysis. *Medical engineering & physics* 2008;30(3):350–7.
- [267] Obermeyer Z, Lee TH. Lost in thought: The limits of the human mind and the future of medicine. *The New England journal of medicine* 2017;377(13):1209.
- [268] Jiang F, Jiang Y, Zhi H, Dong Y, Li H, Ma S, et al. Artificial intelligence in healthcare: past, present and future. *Stroke and vascular neurology* 2017;2(4):230–43.
- [269] Schmidt-Erfurth U, Sadeghipour A, Gerendas BS, Waldstein SM, Bogunovi´c H. Artificial intelligence in retina. *Progress in retinal and eye research* 2018;67:1–29.
- [270] Joshi S, Karule P. A review on exudates detection methods for diabetic retinopathy. *Biomedicine & Pharmacotherapy* 2018;97:1454–60.
- [271] Almotiri J, Elleithy K, Elleithy A. Retinal vessels segmentation techniques and algorithms: a survey. *Applied Sciences* 2018;8(2):155.
- [272] Almazroa A, Burman R, Raahemifar K, Lakshminarayanan V. Optic disc and optic cup segmentation methodologies for glaucoma image detection: a survey. *Journal of ophthalmology* 2015;2015.
- [273] Thakur N, Juneja M. Survey on segmentation and classification approaches of optic cup and optic disc for diagnosis of glaucoma. *Biomedical Signal Processing and Control* 2018;42:162–89.
- [274] Litjens G, Kooi T, Bejnordi BE, Setio AAA, Ciompi F, Ghafoorian M, et al. A survey on deep learning in medical image analysis. *Medical image analysis* 2017;42:60–88.

- [275] Khojasteh P, Aliahmad B, Kumar DK. Fundus images analysis using deep features for detection of exudates, hemorrhages and microaneurysms. *BMC ophthalmology* 2018;18(1):1–13.
- [276] Parmar R, Lakshmanan R, Purushotham S, Soundrapandiyan R. Detecting diabetic retinopathy from retinal images using cuda deep neural network. *Intelligent Pervasive Computing Systems for Smarter Healthcare* 2019;:379–96.
- [277] Quellec G, Charrière K, Boudi Y, Cochener B, Lamard M. Deep image mining for diabetic retinopathy screening. *Medical image analysis* 2017;39:178–93.
- [278] Zhou L, Zhao Y, Yang J, Yu Q, Xu X. Deep multiple instance learning for automatic detection of diabetic retinopathy in retinal images. *IET Image Processing* 2017;12(4):563–71.
- [279] Gargeya R, Leng T. Automated identification of diabetic retinopathy using deep learning. *Ophthalmology* 2017;124(7):962–9.
- [280] Son J, Shin JY, Kim HD, Jung KH, Park KH, Park SJ. Development and validation of deep learning models for screening multiple abnormal findings in retinal fundus images. *Ophthalmology* 2020;127(1):85–94.
- [281] Kathiresan S, Sait ARW, Gupta D, Lakshmanaprabu S, Khanna A, Pandey HM. Automated detection and classification of fundus diabetic retinopathy images using synergic deep learning model. *Pattern Recognition Letters* 2020;.
- [282] Abramoff MD, Lou Y, Erginay A, Clarida W, Amelon R, Folk JC, et al. Improved automated detection of diabetic retinopathy on a publicly available dataset through integration of deep learning. *Investigative ophthalmology & visual science* 2016;57(13):5200–6.
- [283] Wang Z, Yin Y, Shi J, Fang W, Li H, Wang X. Zoom-in-net: Deep mining lesions for diabetic retinopathy detection. In: *International Conference on Medical Image Computing and Computer-Assisted Intervention*. Springer; 2017, p. 267–75.
- [284] Lam C, Yu C, Huang L, Rubin D. Retinal lesion detection with deep learning using image patches. *Investigative ophthalmology & visual science* 2018;59(1):590–6.

- [285] Sayres R, Taly A, Rahimy E, Blumer K, Coz D, Hammel N, et al. Using a deep learning algorithm and integrated gradients explanation to assist grading for diabetic retinopathy. *Ophthalmology* 2019;126(4):552–64.
- [286] Maji D, Santara A, Mitra P, Sheet D. Ensemble of deep convolutional neural networks for learning to detect retinal vessels in fundus images. *arXiv preprint arXiv:160304833* 2016;.
- [287] Maninis KK, Pont-Tuset J, Arbeláez P, Van Gool L. Deep retinal image understanding. In: *International conference on medical image computing and computer-assisted intervention*. Springer; 2016, p. 140–8.
- [288] Dasgupta A, Singh S. A fully convolutional neural network based structured prediction approach towards the retinal vessel segmentation. In: *2017 IEEE 14th International Symposium on Biomedical Imaging (ISBI 2017)*. IEEE; 2017, p. 248–51.
- [289] Fu H, Xu Y, Wong DWK, Liu J. Retinal vessel segmentation via deep learning network and fully-connected conditional random fields. In: *2016 IEEE 13th international symposium on biomedical imaging (ISBI)*. IEEE; 2016, p. 698–701.
- [290] Mo J, Zhang L. Multi-level deep supervised networks for retinal vessel segmentation. *International journal of computer assisted radiology and surgery* 2017;12(12):2181–93.
- [291] Lahiri A, Roy AG, Sheet D, Biswas PK. Deep neural ensemble for retinal vessel segmentation in fundus images towards achieving label-free angiography. In: *2016 38th Annual International Conference of the IEEE Engineering in Medicine and Biology Society (EMBC)*. IEEE; 2016, p. 1340–3.
- [292] Li Q, Feng B, Xie L, Liang P, Zhang H, Wang T. A cross-modality learning approach for vessel segmentation in retinal images. *IEEE Transactions on Medical Imaging* 2015;35(1):109–18.
- [293] Lim G, Cheng Y, Hsu W, Lee ML. Integrated optic disc and cup segmentation with deep learning. In: *2015 IEEE 27th International Conference on Tools with Artificial Intelligence (ICTAI)*. IEEE; 2015, p. 162–9.
- [294] Zhang D, Zhu W, Zhao H, Shi F, Chen X. Automatic localization and segmentation of optical disk based on faster r-cnn and level set in fundus image. In: *Medical Imaging 2018: Image Processing*; vol. 10574. International Society for Optics and Photonics; 2018, p. 105741U.

- [295] Sevastopolsky A. Optic disc and cup segmentation methods for glaucoma detection with modification of u-net convolutional neural network. *Pattern Recognition and Image Analysis* 2017;27(3):618–24.
- [296] Alghamdi HS, Tang HL, Waheeb SA, Peto T. Automatic optic disc abnormality detection in fundus images: A deep learning approach 2016;.
- [297] Haloi M. Improved microaneurysm detection using deep neural networks. arXiv preprint arXiv:150504424 2015;.
- [298] Chudzik P, Majumdar S, Caliva F, Al-Diri B, Hunter A. Microaneurysm detection using fully convolutional neural networks. *Computer methods and programs in biomedicine* 2018;158:185–92.
- [299] Shan J, Li L. A deep learning method for microaneurysm detection in fundus images. In: 2016 IEEE First International Conference on Connected Health: Applications, Systems and Engineering Technologies (CHASE). IEEE; 2016, p. 357–8.
- [300] Lahmiri S. Hybrid deep learning convolutional neural networks and optimal nonlinear support vector machine to detect presence of hemorrhage in retina. *Biomedical Signal Processing and Control* 2020;60:101978.
- [301] Derwin DJ, Selvi ST, Singh OJ. Secondary observer system for detection of microaneurysms in fundus images using texture descriptors. *Journal of Digital Imaging* 2020;33(1):159–67.
- [302] Gondal WM, Köhler JM, Grzeszick R, Fink GA, Hirsch M. Weakly-supervised localization of diabetic retinopathy lesions in retinal fundus images. In: 2017 IEEE international conference on image processing (ICIP). IEEE; 2017, p. 2069–73.
- [303] Benzamin A, Chakraborty C. Detection of hard exudates in retinal fundus images using deep learning. In: 2018 Joint 7th International Conference on Informatics, Electronics & Vision (ICIEV) and 2018 2nd International Conference on Imaging, Vision & Pattern Recognition (icIVPR). IEEE; 2018, p. 465–9.
- [304] Prentasic P, Loncaric S. Detection of exudates in fundus photographs using deep neural networks and anatomical landmark detection fusion. *Computer methods and programs in biomedicine* 2016;137:281–92.

- [305] Asiri N, Hussain M, Al Adel F, Alzaidi N. Deep learning based computer-aided diagnosis systems for diabetic retinopathy: A survey. *Artificial intelligence in medicine* 2019;.
- [306] Simonyan K, Zisserman A. Very deep convolutional networks for large-scale image recognition. *arXiv preprint arXiv:14091556* 2014;.